

UC Berkeley

UC Berkeley Previously Published Works

Title

Search for Higgs boson pair production in the $\gamma\gamma WW^*$ channel using pp collision data recorded at $s=13$ TeV with the ATLAS detector

Permalink

<https://escholarship.org/uc/item/1fh5w57z>

Journal

European Physical Journal C, 78(12)

ISSN

1434-6044

Authors

Aaboud, M

Aad, G

Abbott, B

et al.

Publication Date

2018-12-01

DOI

10.1140/epjc/s10052-018-6457-x

Peer reviewed

Search for Higgs boson pair production in the $\gamma\gamma WW^*$ channel using pp collision data recorded at $\sqrt{s} = 13$ TeV with the ATLAS detector

ATLAS Collaboration*

CERN, 1211 Geneva 23, Switzerland

Received: 24 July 2018 / Accepted: 14 November 2018 / Published online: 11 December 2018
© CERN for the benefit of the ATLAS collaboration 2018

Abstract Searches for non-resonant and resonant Higgs boson pair production are performed in the $\gamma\gamma WW^*$ channel with the final state of $\gamma\gamma\ell\nu jj$ using 36.1 fb^{-1} of proton–proton collision data recorded at a centre-of-mass energy of $\sqrt{s} = 13$ TeV by the ATLAS detector at the Large Hadron Collider. No significant deviation from the Standard Model prediction is observed. A 95% confidence-level observed upper limit of 7.7 pb is set on the cross section for non-resonant production, while the expected limit is 5.4 pb. A search for a narrow-width resonance X decaying to a pair of Standard Model Higgs bosons HH is performed with the same set of data, and the observed upper limits on $\sigma(pp \rightarrow X) \times B(X \rightarrow HH)$ range between 40.0 and 6.1 pb for masses of the resonance between 260 and 500 GeV, while the expected limits range between 17.6 and 4.4 pb. When deriving the limits above, the Standard Model branching ratios of the $H \rightarrow \gamma\gamma$ and $H \rightarrow WW^*$ are assumed.

1 Introduction

A particle consistent with the Standard Model (SM) Higgs boson (H) was discovered by both the ATLAS and CMS experiments at the Large Hadron Collider (LHC) in 2012 [1, 2]. Various studies of its properties have been performed [3–7], and no significant deviation from the SM predictions has been found. The SM Higgs boson is a strong probe of physics beyond the SM. This paper documents searches for both non-resonant and resonant production of Higgs boson pairs (HH) in the semileptonic $\gamma\gamma WW^*$ final state using 36.1 fb^{-1} of proton–proton (pp) collision data recorded by the ATLAS detector at a centre-of-mass energy of $\sqrt{s} = 13$ TeV. Previous searches for Higgs boson pair production have been performed by both the ATLAS and CMS experiments with data recorded at $\sqrt{s} = 8$ TeV in the final states $b\bar{b}b\bar{b}$ [8], $b\bar{b}\gamma\gamma$ [9, 10], $b\bar{b}\tau^+\tau^-$ [11–13] and $\gamma\gamma WW^*$ [11], as well as

multi-lepton and multi-photon [14]. The pp collision data at $\sqrt{s} = 13$ TeV have been analysed in order to search for Higgs boson pairs in the final states $b\bar{b}b\bar{b}$ [15] and $b\bar{b}WW^*$ [16]. No significant excess was observed compared to the SM prediction. However, it is important to explore the 13 TeV data in the channels that are not covered yet, such as the $\gamma\gamma WW^*$ channel presented in this paper. Although this decay channel is not the most sensitive amongst all possible Higgs boson decays, it relies on the Higgs boson couplings to vector bosons, which are already relatively well measured. Furthermore, this channel will contribute to the final combination of all measurable HH decays.

The SM prediction of the Higgs boson pair production cross section is several orders of magnitude smaller than the single-Higgs-boson production rate [17], due to additional ttH or HHH vertices, an additional on-shell Higgs boson that reduces the kinematic phase space, and the fact that the two leading-order (LO) Feynman diagrams have strong destructive interference [18]. In Fig. 1a, the so-called box diagram represents Higgs boson pair production via a heavy-quark loop, where the cross section scales with the squared value of the ttH or bbH coupling constants. In Fig. 1b, the so-called triangle diagram contributes to Higgs boson pair production via the exchange of a virtual Higgs boson and is the only tree-level diagram sensitive to the Higgs boson self-coupling constant (λ_{HHH}), the squared value of which scales the cross section.

In many beyond-the-SM (BSM) scenarios, Higgs boson pair production can be enhanced by modifying the ttH , bbH or λ_{HHH} coupling constants from their SM values, reducing the effect of the destructive interference [19] between Fig. 1a and Fig. 1b, or by replacing the virtual Higgs boson with an intermediate scalar resonance, cf. Fig. 1c. Various BSM models with extended Higgs sectors predict a heavy Higgs boson decaying into a pair of Higgs bosons similar to the one in the SM. Such models include the two-Higgs-doublet models (2HDM) [20], the minimal supersymmetric extension of the SM [21], twin Higgs models [22] and composite

* e-mail: atlas.publications@cern.ch

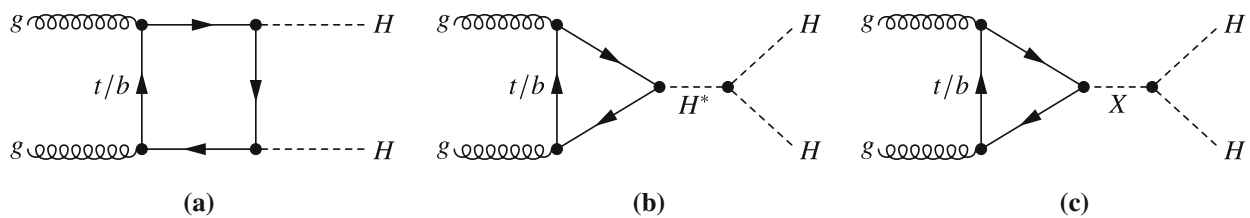


Fig. 1 Feynman diagrams for leading-order Higgs boson pair production in the SM through **a** a heavy-quark loop, **b** the Higgs self-coupling, and **c** an intermediate heavy resonance in a BSM scenario. The total SM contribution is the sum of the two modes depicted in **a** and **b**, which

have significant destructive interference. Physics beyond the SM can enhance Higgs boson pair production either by modifying the Higgs boson coupling constants from their SM values in **a** and/or **b**, or by an additional s-channel exchange of an intermediate scalar resonance in **c**

Higgs models [23,24]. Heavy resonances, other than heavy Higgs bosons, that can decay into a pair of SM Higgs bosons, are predicted in different models, and could for instance be gravitons [25], radions [26] or stoponium [27].

This paper reports searches for non-resonant and resonant production of pairs of Higgs bosons in the semileptonic $\gamma\gamma WW^*$ final state ($\gamma\gamma\ell\nu jj$), i.e. with two photons, two jets, one charged lepton and a neutrino. This final state benefits from the large branching fraction of $H \rightarrow WW^*$ [17], a characteristic signature from two photons and one lepton, as well as the excellent resolution of the diphoton invariant mass $m_{\gamma\gamma}$, which provides good discrimination from a smooth continuum background composed of multi-photon and multi-jet SM processes. Given the expected sensitivity in 13 TeV data, the di-Higgs-boson mass range between 260 and 500 GeV is explored in the search for a scalar resonant Higgs boson pair production.

2 The ATLAS detector

The ATLAS experiment [28] is a multipurpose particle detector with a forward-backward symmetric cylindrical geometry and nearly 4π coverage in solid angle.¹ It consists of an inner tracking detector (ID) surrounded by a thin superconducting solenoid providing a 2 T axial magnetic field, electromagnetic (EM) and hadronic calorimeters, and a muon spectrometer (MS). The ID covers the pseudorapidity range $|\eta| < 2.5$ and consists of silicon pixel, silicon microstrip, and transition-radiation tracking systems. The innermost pixel layer, the insertable B-layer [29], was installed at a mean radius of 3.3 cm after Run 1, and has been operational since

¹ ATLAS uses a right-handed coordinate system with its origin at the nominal interaction point (IP) in the centre of the detector and the z axis along the beam pipe. The x axis points from the IP to the centre of the LHC ring, and the y axis points upwards. Cylindrical coordinates (r, ϕ) are used in the transverse plane, ϕ being the azimuthal angle around the z-axis. The pseudorapidity is defined in terms of the polar angle θ as $\eta = -\ln \tan(\theta/2)$. Angular distance is measured in units of $\Delta R \equiv \sqrt{(\Delta\eta)^2 + (\Delta\phi)^2}$.

the beginning of Run 2. Lead/liquid-argon (LAr) EM sampling calorimeters with high granularity provide energy measurements of EM showers. A steel/scintillator-tile hadronic calorimeter covers the central pseudorapidity range ($|\eta| < 1.7$). The endcap and forward regions are covered by LAr calorimeters for EM and hadronic energy measurements up to $|\eta| = 4.9$. The MS surrounds the calorimeters and is based on three large air-core toroid superconducting magnets with eight coils each and with bending power in the range 2.0–7.5 T m. It includes a system of fast detectors for triggering purposes and precision tracking chambers. A dedicated two-level trigger system is used to select events [30]. The first-level trigger is implemented in hardware and uses a subset of the detector information to reduce the accepted event rate to at most 100 kHz. This is followed by a software-based trigger level that reduces the accepted event rate to an average of 1 kHz.

3 Data and simulated samples

3.1 Data samples

The full set of pp collision data collected during 2015 and 2016 are used in this analysis. The two datasets were recorded at the same centre-of-mass energy $\sqrt{s} = 13$ TeV, albeit with different beam conditions. Beam intensities in 2016 were typically higher than in 2015, resulting in a higher instantaneous luminosity and a larger number of pp collisions in each bunch crossing. The integrated luminosity of the combined 2015+2016 dataset used in this analysis is $36.1 \pm 0.8 \text{ fb}^{-1}$. This dataset were collected in run periods during which all subsystems were operational. The events are collected with a trigger requiring the presence of at least two photons, one with a transverse energy $E_T > 35$ GeV and the second with $E_T > 25$ GeV, and the longitudinal and transverse profiles of the EM shower were required to be consistent with those expected for a photon. The corresponding trigger efficiency reaches about 99% for the events that pass the event selection of the analysis.

Table 1 Simulated signal samples

Processes	Generator	Parton shower	Tune	PDF
Non-resonant	MADGRAPH5_AMC@NLO 2.2.3	HERWIG++	UEEE5	CTEQ6L1
Resonant	MADGRAPH5_AMC@NLO 2.2.3	HERWIG++	UEEE5	CTEQ6L1

3.2 Simulated event samples

Simulated Monte Carlo (MC) samples are used to estimate the signal acceptance and study the modelling for both non-resonant SM Higgs boson pair production and resonant BSM Higgs boson pair production. MC samples are also used to estimate the acceptance and study the modelling for SM single-Higgs-boson production processes, and to study the modelling of the SM continuum background from events with multiple photons and jets (Sect. 5), which is the dominant background in the analysis. Eventually, it is estimated by a data-driven method for both its normalisation and shape.

The simulated samples for signals are listed in Table 1. The event generator MADGRAPH5_AMC@NLO 2.2.3 [31] was used for the production of non-resonant [32] and resonant [33] signal MC samples at next-to-leading order (NLO) in QCD, where four values of the resonance mass ($m_X = 260, 300, 400$ and 500 GeV) are considered. The events were generated by a Higgs Effective Field Theory (HEFT) using the MC@NLO method [34] and were reweighted in order to take into account the effects of the finite top-quark mass. The parton shower was implemented using HERWIG++ 2.7.1 [35] with a set of tuned underlying-event parameters called the UEEE5 tune² [36], and the parton distribution function (PDF) set CTEQ6L1 [37] was used.

- For non-resonant Higgs boson pair production, the inclusive cross sections are normalised to the SM prediction of 33.41 fb [17, 38], calculated at NNLO in QCD, including resummation of soft-gluon emission at next-to-next-to-leading-logarithmic (NNLL) accuracy, as prescribed by the LHC Higgs Cross Section Working Group [17]. The effect of the finite top-quark mass is also taken into account at NLO [39].
- For resonant Higgs boson pair production, a narrow decay width, which is negligible compared to the experimental mass resolution, is assumed. The interference between non-resonant and resonant Higgs boson pair production is implemented in the generator. The interference is minimal and remains negligible when a narrow decay width is assumed.

Table 2 lists the simulated samples for the dominant SM single-Higgs-boson production modes: gluon–gluon fusion

² The tune parameters can be found at the following link: <https://herwig.hepforge.org/tutorials/mpi/tunes.html>.

(ggF), vector-boson fusion (VBF), associated production with a W or Z boson (VH), and associated production with a pair of top quarks ($t\bar{t}H$). For all these processes, the PYTHIA 8.186 parton shower is used for the modelling of non-perturbative effects. The AZNLO tune [40] is used in ggF, VBF and VH simulations, while the A14 tune is used in $t\bar{t}H$ simulations.

- **gluon–gluon fusion:** The ggF production is accurate to NNLO in QCD, using the POWHEG method [41] for matching the matrix element with the parton shower, and the MiNLO method [42, 43] to simultaneously achieve NLO accuracy for inclusive Higgs boson production. Furthermore, a reweighting procedure was performed using the HNNLO program [44–46] to achieve full NNLO accuracy [47]. This sample is referred to as NNLOPS. The PDF4LHC15 NLO PDF set [48] was used. The inclusive cross section of the ggF production is normalised to the calculation at next-to-next-to-next-to-leading-order (N^3 LO) QCD and NLO electroweak (EW) accuracies [49].
- **VBF and VH :** VBF and VH production was simulated at NLO in QCD with POWHEG-BOX v2 [41, 50, 51] using the PDF4LHC15 NLO PDF set. The inclusive VBF contribution is normalised to the cross section calculated with NLO QCD and NLO EW corrections [52–54] with an approximate NNLO QCD correction applied [55]. The contributions are normalised to cross sections calculated with NNLO QCD [56] and NLO EW corrections [57] for WH and $q\bar{q} \rightarrow ZH$ and at NLO and next-to-leading-logarithm (NLL) accuracy in QCD for $gg \rightarrow ZH$ [58].
- **$t\bar{t}H$:** The $t\bar{t}H$ production is simulated using MADGRAPH5_AMC@NLO 2.2.3 and its inclusive cross section is normalised to a calculation with NLO QCD and NLO EW corrections [59–62].

Processes of continuum backgrounds of multiple photons and jets with either one or zero leptons were simulated with MADGRAPH5_AMC@NLO 2.2.2, interfaced with the parton shower model in PYTHIA 8.186.

Multiple pp collisions in each bunch crossing, “pile-up”, were simulated with the soft QCD processes of PYTHIA 8.186 using the A2 tune [63] and the MSTW2008LO PDF set [64]. An additional event-level reweighting is performed in order to ensure that the distribution of the average number of interactions per bunch crossing matches that occur-

Table 2 Simulated SM single-Higgs-boson background samples with $m_H = 125$ GeV

Processes	Generators	QCD order	EW order	PDF	Parton shower	Normalisation
ggF	POWHEG NNLOPS	NNLO	NLO	PDF4LHC15	PYTHIA 8.186	N ³ LO (QCD) + NLO (EW)
VBF	POWHEG	NLO	NLO	PDF4LHC15	PYTHIA 8.186	NNLO (QCD) + NLO (EW)
W^+H	POWHEG MiNLO	NLO	NLO	PDF4LHC15	PYTHIA 8.186	NNLO (QCD) + NLO (EW)
W^-H	POWHEG MiNLO	NLO	NLO	PDF4LHC15	PYTHIA 8.186	NNLO (QCD) + NLO (EW)
$q\bar{q} \rightarrow ZH$	POWHEG MiNLO	NLO	NLO	PDF4LHC15	PYTHIA 8.186	NNLO (QCD) + NLO (EW)
$ggZH$	POWHEG MiNLO	NLO	NLO	PDF4LHC15	PYTHIA 8.186	NLO NLL (QCD)
$t\bar{t}H$	MADGRAPH AMC@NLO	NLO	NLO	NNPDF3.0	PYTHIA 8.186	NLO (QCD) + NLO (EW)

ring in the data used in this analysis. The particles in the final states of the generated processes were passed through either a GEANT4 [65] simulation of the ATLAS detector, or through the ATLAS fast simulation framework [66], which has been extensively validated against the GEANT4 simulation model. The output from the detector simulation is then analysed using the same reconstruction software as the data. The MC samples for single-Higgs-boson production were simulated with the GEANT4 framework, while the other samples used in this analysis were produced with the ATLAS fast simulation framework.

4 Object and event selection

The event selection is based on the properties of the visible objects in the final state, which includes one charged lepton (electron or muon), two jets, and two photons. These objects are reconstructed from detector-level objects, such as energy clusters in the EM calorimeter and tracks in the ID, as well as in the MS.

4.1 Object reconstruction

Photon candidates are reconstructed from clusters of energy deposited in the EM calorimeter [67]. If the candidates are matched with a reconstructed conversion vertex or tracks consistent with the hypothesis of a $\gamma \rightarrow e^+e^-$ conversion, they are classified as converted photon candidates.³ If the matched track is consistent with the hypothesis of an electron produced in the beam interaction region, they are classified as electron candidates. If the candidates are not matched with a reconstructed conversion vertex or tracks satisfying the conversion requirement, they are classified as unconverted photon candidates. The energy is determined by summing the energies of all cells that belong to the associated cluster [68] and is corrected using a combination of simulation-based

and data-driven calibration factors [69] determined from $Z \rightarrow e^+e^-$ events collected in 2015 and 2016. The photon energy resolution in simulation is corrected to match the resolution in data [67]. The reconstructed photon candidates are required to meet “tight” photon identification criteria [68], which are based on the lateral and longitudinal energy profiles of EM showers in the calorimeter. The identification efficiency is measured as a function of the transverse energy of photons (E_T^γ). It ranges from 90 to 98% for converted photons and from 85 to 95% for unconverted photons, in the E_T^γ interval between 25 and 200 GeV. To suppress the background from jets misidentified as photons, all reconstructed photon candidates are required to meet a set of calorimeter- and track-based isolation criteria [70]. A calorimeter-based isolation variable E_T^{iso} is defined as the sum of the transverse energies (E_T) of all positive-energy topological clusters of calorimeter cells [71] within $\Delta R = 0.2$ of the photon candidate, excluding the energy of the photon candidate itself. The selection applied to the calorimeter-based isolation variable is $E_T^{\text{iso}} < 0.065 E_T^\gamma$. A track-based isolation variable p_T^{iso} is defined as the scalar sum of the transverse momenta (p_T) of tracks with $p_T > 1$ GeV within $\Delta R = 0.2$ of the photon candidate, excluding tracks from photon conversions. The selection on the track-based isolation variable is $p_T^{\text{iso}} < 0.05 E_T^\gamma$. Only photon candidates with $|\eta| < 2.37$ are considered, excluding the transition region between the barrel and endcap calorimeters ($1.37 < |\eta| < 1.52$).

Electron candidates are reconstructed from clusters of energy deposited in the EM calorimeter matched to a track in the inner detector, as described above. A likelihood-based (LH) algorithm is used [72] to perform the electron identification against the background from jets or non-prompt electrons. Electron candidates are identified according to the “medium LH” criteria. Muon candidates are identified by matching a reconstructed ID track with a reconstructed MS track [73]. The identification classifies muon candidates as either “loose” or “medium”, based on the number of hits in the different ID and MS subsystems, and on the significance of the difference $|q/p_{\text{MS}} - q/p_{\text{ID}}|$, where q is the

³ Converted photons are those that convert to an e^+e^- pair inside the ID volume, with at least one of the two lepton trajectories reconstructed, while unconverted photons directly enter the EM calorimeter.

charge and p is the momentum of the muon candidate, as well as on the energy deposit in the tile hadronic calorimeters. The “medium” candidates are used in the analysis. An efficiency ranging from 84 to 93% as a function of E_T or p_T is achieved in the combined identification and reconstruction of electrons, and 96% (above 98%) in muon identification (reconstruction), in the range where the objects are selected. The electron (muon) is required to pass the “Loose” (“GradientLoose”) isolation criterion based on the sum of p_T of tracks lying within a cone of $\Delta R = \min(10 \text{ GeV}/p_T^{e(\mu)}, 0.3)$ and the sum of E_T of topological clusters of calorimeter cells within a cone of $\Delta R = 0.2$ (0.2) around the electron (muon) candidate, excluding the contributions from the electron (muon) candidate. With these requirements the isolation efficiencies for electrons (muons) are above 99% ($0.057p_T^\mu + 95.57\%$) [72, 73]. Finally, the electron candidates are required to have $E_T > 10 \text{ GeV}$ and $|\eta| < 2.47$, excluding the transition region between the barrel and endcap calorimeters ($1.37 < |\eta| < 1.52$), whereas the muon candidates are required to have $p_T > 10 \text{ GeV}$ and $|\eta| < 2.7$.

Jets are reconstructed via the FastJet package [74] using the anti- k_t clustering algorithm [75] with a radius parameter $R = 0.4$. The jet energies are determined at the EM scale and calibrated using particle-level correction factors based on a combination of simulation and data [76–80]. Jets are required to have $|\eta| < 2.5$ and $p_T > 25 \text{ GeV}$. In addition, a jet-vertex tagging algorithm (JVT) [81] is applied to jets with $|\eta| < 2.4$ and $p_T < 60 \text{ GeV}$ in order to suppress jets originating from pile-up interactions. In this algorithm, a multivariate discriminant based on two track-based variables is constructed to reject pile-up jets while maintaining a high efficiency for the hard-scatter jet independent of the number of primary vertices in the event. The selected jets are classified as b -jets using a multivariate technique [82, 83], which takes advantage of the information about secondary vertices, the impact parameters of the associated tracks and the topologies of decays of heavy-flavour hadrons. The b -tagging working point is selected to have an efficiency of 70% for a b -jet from $t\bar{t}$ decays, with a rejection factor of 12 for jets originating from c -quarks (c -jets), and of close to 400 for jets initiated by light-flavour quarks or gluons (light-flavour jets).

An overlap removal procedure is performed in the following order to avoid double counting of detector-level objects when reconstructing physics objects. Electrons with $\Delta R(e, \gamma) < 0.4$ are removed. Jets with $\Delta R(\text{jet}, \gamma) < 0.4$ or $\Delta R(\text{jet}, e) < 0.2$ are removed. Electrons with $\Delta R(e, \text{jet}) < 0.4$ are removed. Muons with $\Delta R(\mu, \gamma) < 0.4$ or $\Delta R(\mu, \text{jet}) < 0.4$ are removed.

4.2 Event selection

The events passing the diphoton trigger are required to contain at least two jets, no b -jet, and at least one charged lepton (e or μ , but including contributions from fully leptonic τ -lepton decays) in the final state. The two photon candidates with the leading (sub-leading) E_T are required to satisfy $E_T^\gamma/m_{\gamma\gamma} > 0.35$ (0.25). The b -jet veto suppresses the $t\bar{t}H$ process. Furthermore, the transverse momentum of the diphoton system ($p_T^{\gamma\gamma}$) is required to be larger than 100 GeV for maximising the sensitivity and keeping at least 70% of signal events. This requirement suppresses continuum background events when searching for non-resonant Higgs boson pair production, or resonant production with resonance masses of 400 GeV or higher. However, the $p_T^{\gamma\gamma}$ selection is omitted in the search for resonance masses below 400 GeV due to a limited separation between signal and continuum background in this kinematical region, as can be seen in Fig. 2. These final selection criteria, together with a requirement on the invariant diphoton mass of $105 \text{ GeV} < m_{\gamma\gamma} < 160 \text{ GeV}$, define the event sample on which the signal search is performed for the various assumed signal models. A data “sideband” sample is selected applying the same criteria, but excluding the Higgs mass region $m_{\gamma\gamma}$ 121.7–128.5 GeV, and can be used together with other samples to study the continuum background.

If there were an observable signal, one of the Higgs bosons would be directly visible in the $m_{\gamma\gamma}$ distribution. The combination of two jets and at least one charged lepton would be consistent with $H \rightarrow WW^*$ for the other Higgs boson. Its signature would in principle be enhanced by a missing transverse energy (E_T^{miss}) requirement to indicate a neutrino, but a selection on E_T^{miss} was found not to produce any significant improvement in sensitivity, and so was not applied. The magnitude of E_T^{miss} [84, 85] is measured from the negative vectorial sum of the transverse momenta of all photon, electron and muon candidates and of all hadronic jets after accounting for overlaps between jets, photons, electrons, and muons, as well as an estimate of soft contributions based on tracks.

After all selections described above, the combined acceptance and selection efficiency for non-resonant production is 8.5%, while it ranges from 6.1 to 10% as a function of the mass of the resonance (m_X) from 260 to 500 GeV, as shown in Table 3. The efficiency for the non-resonant Higgs boson pair production is at the same level as the efficiency for the high-mass resonant production, as the Higgs bosons and their decay products tend to exhibit large transverse momenta due to the box diagram shown in Fig. 1a.

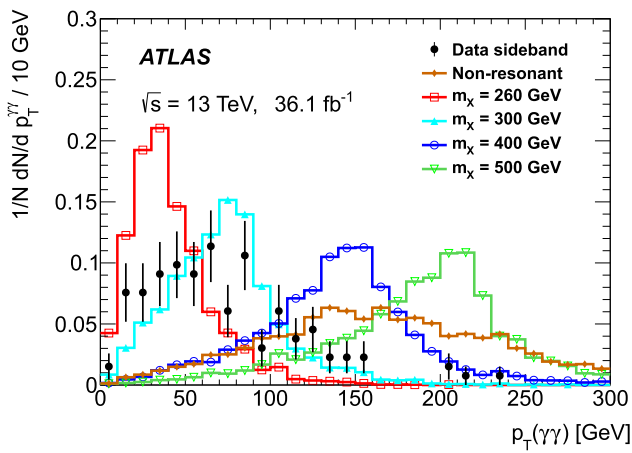


Fig. 2 Distributions of the reconstructed transverse momenta of the diphoton system with all event selections, except the $p_T^{\gamma\gamma}$ selection, applied for various signal models, as well as sideband data, normalised to unit area

Table 3 The combined acceptance and efficiency for non-resonant and resonant with different scalar resonance masses m_X , with and without a $p_T^{\gamma\gamma}$ selection

	No $p_T^{\gamma\gamma}$ selection			$p_T^{\gamma\gamma} > 100$ GeV		
m_X (GeV)	260	300	400	400	500	Non-resonant
Acceptance × efficiency (%)	6.1	7.1	9.7	7.8	10	8.5

5 Signal and background estimation

A fit to the $m_{\gamma\gamma}$ distribution is performed to extract the signal yield as described in Sect. 7. The shapes of both the signal and background distributions are modelled with analytical functions. For both Higgs boson pair production and single-Higgs-boson processes, the $m_{\gamma\gamma}$ distributions are modelled with double-sided Crystal Ball functions [86]. Their shape parameters are determined by a fit to simulated samples. The single-Higgs-boson contribution is normalised to the SM cross-sections as described in Sect. 3.2. Higgs boson pair production is regarded as a background to the resonant search. Its contribution is also set to the SM prediction of Sect. 3.2.

The continuum background is modelled with an exponential function of a second-order polynomial. Several functional forms were evaluated by fitting the sidebands in data and MC samples under different conditions of photon purity and lepton multiplicity. Photon purity was lowered, compared to the final data selection, by reversing the requirements on photon isolation or identification. For higher photon purity, MC samples with prompt photons were used. The lepton multiplicity was varied to be zero or at least one. For all combinations of conditions, the exponential function with a second-order polynomial gave the best fits, with satisfactory χ^2 , and was chosen to model the continuum background.

Table 4 Numbers of expected and observed events in the $m_H \pm 2 \sigma_{m_{\gamma\gamma}}$ mass window with or without a $p_T^{\gamma\gamma}$ selection. A cross section of 33.41 fb is assumed for non-resonant Higgs boson pair production when it is considered as a background in resonant searches. The resulting yields are determined from the fit to data by integrating the resulting functional forms over the selected $m_{\gamma\gamma}$ range. The error in each yield includes both the statistical and systematic uncertainties, as discussed in Sect. 6

Process	Number of events	
	No $p_T^{\gamma\gamma}$ selection	$p_T^{\gamma\gamma} > 100$ GeV
Continuum background	22 ± 5	5.1 ± 2.3
SM single-Higgs	1.92 ± 0.15	1.0 ± 0.09
SM di-Higgs	0.046 ± 0.004	0.038 ± 0.004
Sum of expected background	24 ± 5	6.1 ± 2.3
Data	33	7

The shape parameters and normalisation are free to float in the final fit to the data. Since any functional form might introduce spurious signals, this effect is estimated with a sample mixing irreducible prompt-photon background from simulation and reducible backgrounds from data, as described in Sect. 6.

The expected numbers of signal and background events are shown in Table 4 together with the number of events observed in data. Only events within a mass window of $m_H \pm 2 \sigma_{m_{\gamma\gamma}}$ are reported, where the Higgs boson mass (m_H) is taken to be 125.09 GeV [87] and the diphoton mass resolution ($\sigma_{m_{\gamma\gamma}}$) is 1.7 GeV and is obtained from simulation. The dominant background is from continuum processes with multiple photons and jets. A small background arises from SM single-Higgs-boson production processes, among which $t\bar{t}H$ and WH productions give the leading contributions with, respectively, a fraction of 41.5% (39.2%) and 23.3% (22.5%) of the whole single-Higgs-boson contribution with (without) the $p_T^{\gamma\gamma} > 100$ GeV selection.

6 Systematic uncertainties

6.1 Theoretical uncertainties

Theoretical uncertainties in the prediction of the cross section of single Higgs bosons are estimated from variations of the normalisation and factorisation scales, PDF, and the running QCD coupling constant (α_S) [17]. Among the dominant production modes $t\bar{t}H$ and VH , the cross section of $t\bar{t}H$ has the largest uncertainty: up to 9.2% in the scale variations, up to 3.0% in the PDF variations, and 2.0% in the α_S variations, as prescribed by the LHC Higgs Cross Section Working Group [17].

The theoretical uncertainties in the efficiency times acceptance ($\epsilon \times A$) are estimated from scale, PDF and parton shower variations. The scale uncertainty ranges from 2.1 to

4.1% for resonant production and is 3.4% for non-resonant production. The PDF uncertainty is around 2.5 and 3.0% for the resonant and non-resonant production, respectively. The parton shower uncertainty is estimated by comparing PYTHIA 8 and Herwig++ as two different shower models, and ranges from 6.0% at $m_X = 500$ GeV to 29.6% at $m_X = 260$ GeV for resonant production, and is 7.8% for non-resonant production. This uncertainty is large in low-mass resonant production because the jet spectrum at low- p_T is more susceptible to variations in the parton shower model. Non-resonant Higgs boson pair production is considered as a background in the search for resonant Higgs boson pair production. The scale, PDF, α_S and HEFT uncertainties in the calculation of the cross section for SM Higgs boson pair production are also taken into account. These values are 6.0%, 2.1%, 2.3%, and 5.0%, respectively, following the recommendations in Ref. [17]. Further uncertainties arising from the $H \rightarrow \gamma\gamma$ and $H \rightarrow WW^*$ branching ratios (B) are considered as well. They are 2.1% and 1.5% [17], respectively.

6.2 Modelling uncertainties in the continuum background

The exponential function of a second-order polynomial is determined to provide the simplest and most robust functional form for modelling the continuum background as described in Sect. 5. The uncertainties in the modelling are estimated by fitting a signal-plus-background model to a simulated background-only sample that has such a large number of events that its own statistical uncertainty does not affect the test results. The fitted number of signal events (n_{ss}) quantifies spurious signal events. The fits are performed with the assumed m_H ranging from 120 to 130 GeV in steps of 0.5 GeV. The maximum value of the fitted signal yields $|n_{ss}|$ is regarded as a bias in the yields due to the background modelling (the spurious signal), and is, conservatively, taken into account in the fit as the modelling uncertainty. The fitted $|n_{ss}|$ value reaches as large as 0.46 when not applying the $p_T^{\gamma\gamma}$ selection, and 0.26 when applying the selection. The simulated background-only samples include the irreducible process of $\gamma\gamma\ell\nu jj$ and the reducible processes represented by events where one or two hadronic jets are misidentified as photons. The reducible processes are modelled by the data events with reversed photon identification or isolation requirements. The two components are combined according to the measured diphoton purity, which is about 88% (90% with $p_T^{\gamma\gamma}$ selection) and normalised according to the number of selected data events.

6.3 Experimental uncertainties

The uncertainty in the measurement of the combined 2015+2016 integrated luminosity is 2.1%. It is derived, following a methodology similar to that detailed in Ref. [88], from a cal-

ibration of the luminosity scale using x - y beam-separation scans performed in August 2015 and May 2016. All processes that are estimated using simulation are affected by the uncertainty in the luminosity measurement.

The efficiency of the diphoton trigger is estimated using bootstrap methods [89] with a systematic uncertainty of 0.4%. The photon identification uncertainty is obtained by varying the data-to-simulation efficiency corrections within their uncertainties, derived from control samples of photons from radiative Z boson decays and from inclusive γ events, and of electrons from $Z \rightarrow e^+e^-$ decays. A maximal uncertainty of 1.7% in the yields is evaluated in all of the SM single-Higgs-boson, SM di-Higgs-boson and BSM Higgs boson production processes. The photon-track isolation uncertainty is derived from measurements of the uncertainty in the data-to-simulation efficiency corrections using inclusive-photon control samples, while the uncertainty from the calorimeter isolation requirement is evaluated from the difference between applying and not applying corrections derived from inclusive-photon events to the calorimeter isolation variable in the simulation. In general, the overall isolation uncertainty is less than 1%. The uncertainties from the photon energy resolution and scale affect the yields by less than 0.2%. The relevant impact on the shape of the diphoton invariant mass is also considered by introducing variations of the resolution and mean values of the fit function and is estimated using simulation. The photon energy resolution varies the resolution of the $m_{\gamma\gamma}$ shape by 5.2–11.4%, while the photon energy scale affects the mean value by about 0.5%. The jet energy scale (JES) and the corresponding uncertainties are derived from both simulation and in situ calibration using data [77, 90]. This affects the event selection efficiency by 2.4–9.9%, depending on the process. The jet energy resolution (JER) uncertainty is evaluated by smearing jet energies according to the systematic uncertainties of the resolution measurement [80, 91], and its impact on the event selection efficiency ranges from 0.1 to 1.6%. The b -tagging uncertainties is derived separately for b -jets, c -jets and light-flavour jets [82]. Overall, their impact on the yields is not more than 4%. Uncertainties arising from the reconstruction, identification and isolation of both the electron and muon candidates [72, 73], are propagated to the event yield variations, and they are found to have an impact of less than 1%. Finally, the pile-up reweighting procedure, which matches the distribution of the number of interactions per bunch crossing between simulation and data, has associated systematic uncertainties of less than 1%. All experimental uncertainties are correlated among all processes that use simulation to model the yields and the kinematics. A summary of the systematic uncertainties in the expected yields of the di-Higgs-boson and single-Higgs-boson production is presented in Table 5. In the search for non-resonant Higgs boson pair production, SM Higgs boson pair production is

Table 5 Summary of relative systematic uncertainties, in percent, propagated to the yields for the MC-estimated processes. Entries marked by ‘–’ indicate that the systematic uncertainty is not applicable for the corresponding process. The extrapolation uncertainties in *b*-tagging include two components: one is from the extrapolation to high-*p*_T (*p*_T

> 300 GeV) jets and the other one is from extrapolating *c*-jets to *τ*-jets. The values for resonant production shown here assume *m*_X = 260 GeV. Several theoretical uncertainties are reported for the cross section (*σ*) and the combined efficiency and acceptance (*ε* × *A*)

Source of uncertainties	Non-resonant <i>HH</i>	<i>X</i> → <i>HH</i>	Single- <i>H</i> bkg <i>p</i> _T ^{<i>γγ</i>} > 100 GeV	Single- <i>H</i> bkg No <i>p</i> _T ^{<i>γγ</i>} selection
Luminosity 2015 + 2016	2.1	2.1	2.1	2.1
Trigger	0.4	0.4	0.4	0.4
Event sample size	1.7	2.2	1.6	1.3
Pile-up reweighting	0.5	0.9	0.7	0.6
Photon				
Identification	1.7	1.4	0.8	0.8
Isolation	0.8	0.7	0.4	0.4
Energy resolution	0.1	0.1	0.2	< 0.1
Energy scale	0.2	< 0.1	0.2	< 0.1
Jet				
Energy scale	4.0	9.9	2.4	2.6
Energy resolution	0.1	1.6	0.5	1.0
<i>b</i> -tagging				
<i>b</i> -hadron jets	< 0.1	< 0.1	3.8	3.6
<i>c</i> -hadron jets	1.5	1.0	0.7	0.6
Light-flavour jets	0.3	0.3	0.1	0.1
Extrapolation	< 0.1	< 0.1	0.1	< 0.1
Lepton				
Electron	0.5	0.7	0.2	0.2
Muon	0.5	0.7	0.3	0.5
Theory				
PDF on <i>σ</i>	2.1	–	3.4	3.4
<i>α</i> _S on <i>σ</i>	2.3	–	1.3	1.3
Scale on <i>σ</i>	6.0	–	0.9	0.9
HEFT on <i>σ</i>	5.0	–	–	–
Scale on <i>ε</i> × <i>A</i>	2.8	2.5	–	–
PDF on <i>ε</i> × <i>A</i>	3.0	2.4	–	–
Parton shower on <i>ε</i> × <i>A</i>	7.8	29.6	–	–
<i>B</i> (<i>H</i> → <i>γγ</i>)	2.1	2.1	2.1	2.1
<i>B</i> (<i>H</i> → <i>WW</i> *)	1.5	1.5	1.5	1.5
Total	13.6	31.8	7.1	6.8

considered to be the signal process, while single Higgs boson production is considered to be a background. In the search for the resonant Higgs boson pair production, both SM single Higgs boson production and non-resonant Higgs boson pair productions are considered to be background processes.

7 Results

A fit to *m*_{γγ} is performed in the signal region to extract the signal yield. The statistical model is constructed with a likelihood function:

$$\begin{aligned}
 \mathcal{L}(\mu, \theta) = & \prod_i \left((n_{\text{Signal}}(\mu, \theta) + n_{\text{ss}}) \times f_{\text{DSCB}}^1(m_{\gamma\gamma}^i, \theta) \right. \\
 & + n_{\text{Cont}} \times f_{\text{Cont}}(m_{\gamma\gamma}^i, \theta) + n_{\text{SM-one-Higgs}}(\theta) \\
 & \times f_{\text{DSCB}}^2(m_{\gamma\gamma}^i, \theta) + n_{\text{SM-di-Higgs}} \\
 & \left. \times f_{\text{DSCB}}^3(m_{\gamma\gamma}^i, \theta) \right) \prod G(0|\theta, 1) \tag{1}
 \end{aligned}$$

- *i* stands for the event index,
- *n*_{Signal} is the expected number of signal events,
- *μ* is the cross section (times the branching fraction of *X* → *HH*) of non-resonant (resonant) production,

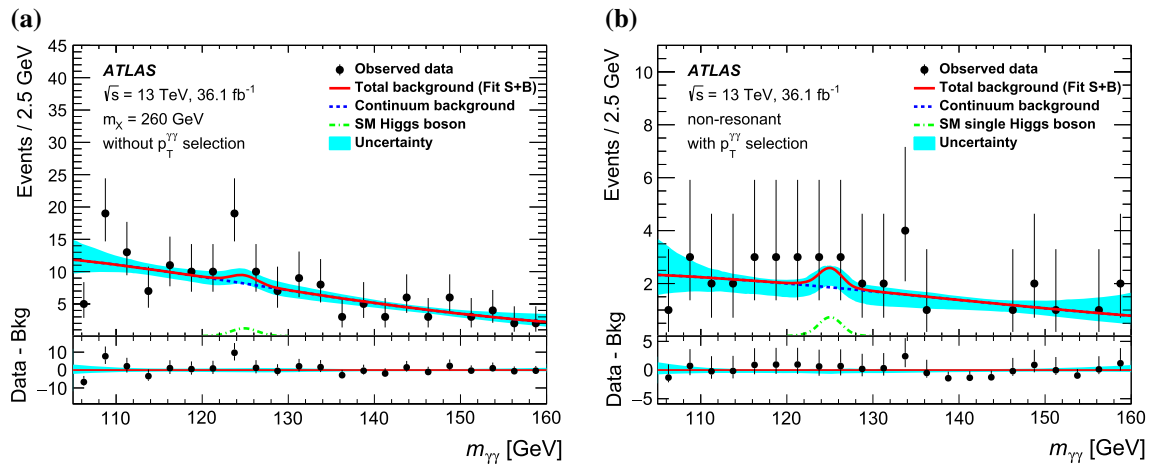


Fig. 3 Invariant mass spectrum of the diphoton system in the searches for both resonant and non-resonant Higgs boson pair production, with the corresponding backgrounds for **a** $m_\chi = 260$ GeV without any $p_T^{\gamma\gamma}$ selection and **b** the non-resonant case with a $p_T^{\gamma\gamma} > 100$ GeV selection. Fits to $m_{\gamma\gamma}$ are performed using the full signal-plus-background model. In each plot, only the background component is present. The shape parameters and normalisation of the continuum background

model are determined in the fits. The “SM Higgs boson” in **a** contains the single-Higgs-boson background and SM di-Higgs-boson background. The band shows the uncertainty of the “Total background” in the upper panel and is calculated by a sampling method. The bottom panel shows the difference between the number of events in data and the estimated number of background events, as determined by the fits

- n_{SS} is the estimated spurious signal yield due to our choice of continuum background modelling,
- f_{DSCB}^1 is the probability density function (pdf) of a double-sided Crystal Ball distribution for signal,
- n_{Cont} is the expected number of continuum background events,
- f_{Cont} is the pdf of the continuum background, i.e. an exponential function of a second-order polynomial,
- $n_{SM-one-Higgs}$ is the expected number of single-Higgs-boson events, which is set to the SM prediction and can vary with uncertainties,
- f_{DSCB}^2 is the pdf of a double-sided Crystal Ball distribution for the SM single-Higgs-boson background,
- $n_{SM-di-Higgs}$ is the expected number of the SM di-Higgs-boson events,
- f_{DSCB}^3 is the pdf of a double-sided Crystal Ball distribution for SM di-Higgs-boson background,
- $G(0|\theta, 1)$ is the pdf of a Gaussian distribution used to constrain the nuisance parameters θ that model systematic uncertainties as introduced in Sect. 6.

Equation (1) is used directly for the BSM resonant signal searches. For the non-resonant SM Higgs boson pair search, the SM Higgs boson pair term is removed.

The distributions in the final signal-plus-background fit using the likelihood function above are shown for two sets of selections separately: in Fig. 3a without requiring the $p_T^{\gamma\gamma}$ selection for masses below 400 GeV, and in Fig. 3b requiring $p_T^{\gamma\gamma} > 100$ GeV for masses above 400 GeV, as well as for the search for non-resonant Higgs boson pair

production. The fits are performed separately on the two distributions to search for resonant signals in both the low-mass and high-mass ranges. The observed data are found to be compatible with the sum of the expected SM backgrounds by performing a likelihood-ratio test [92]. The largest data excess has a local significance of 2.0 standard deviations at 400 GeV without the $p_T^{\gamma\gamma}$ selection. A modified frequentist method CL_s [93] is used to calculate the 95% confidence-level (CL) exclusion limits with the asymptotic approximation [92]. Unfolding the SM Higgs boson branching fractions to WW^* and $\gamma\gamma$ for the signal, the expected upper limit on the cross section for non-resonant Higgs boson pair production is 5.4 pb, while the observed limit is 7.7 pb, as shown in Table 6. The difference between the expected and observed limits is due to a slight excess of events in data. The expected upper limit on the cross section times the branching fraction of $X \rightarrow HH$ ranges from 17.6 to 4.4 pb, while the observed limit ranges from 40 to 6.1 pb, as a function of m_χ between 260 and 500 GeV, as shown in Fig. 4a.

Assuming the SM Higgs branching fractions of $B(H \rightarrow WW^*) = (21.52 \pm 0.32)\%$ and $B(H \rightarrow \gamma\gamma) = (0.227 \pm 0.005)\%$ [17], the expected upper limit on the cross section for non-resonant production of $HH \rightarrow \gamma\gamma WW^*$ is 5.3 fb, while the observed limit is 7.5 fb, as shown in Table 6. The expected upper limit on the cross section for resonant production of $X \rightarrow HH \rightarrow \gamma\gamma WW^*$ ranges from 17.2 to 4.3 fb, while the observed limit ranges from 39.1 to 6.0 fb, as a function of m_χ between 260 and 500 GeV, as shown in Fig. 4b. The statistical uncertainty dominates in the final

Table 6 The 95% CL upper limits for the non-resonant production and the ratios of the limits to the SM cross-section value of $\sigma(pp \rightarrow HH) = 33.4_{-2.8}^{+2.4}$ fb [17]. The $\pm 1\sigma$ and $\pm 2\sigma$ intervals around the median limit are also presented

	+2 σ	+1 σ	Median	-1 σ	-2 σ	Observed
Upper limits on $\sigma(HH)$ (pb)	12	8.0	5.4	3.9	2.9	7.7
Upper limits on $\sigma(HH) \times B(\gamma\gamma WW^*)$ (fb)	12	7.8	5.3	3.8	2.8	7.5
Ratios of limits over the SM $\sigma(HH)$	360	240	160	120	87	230

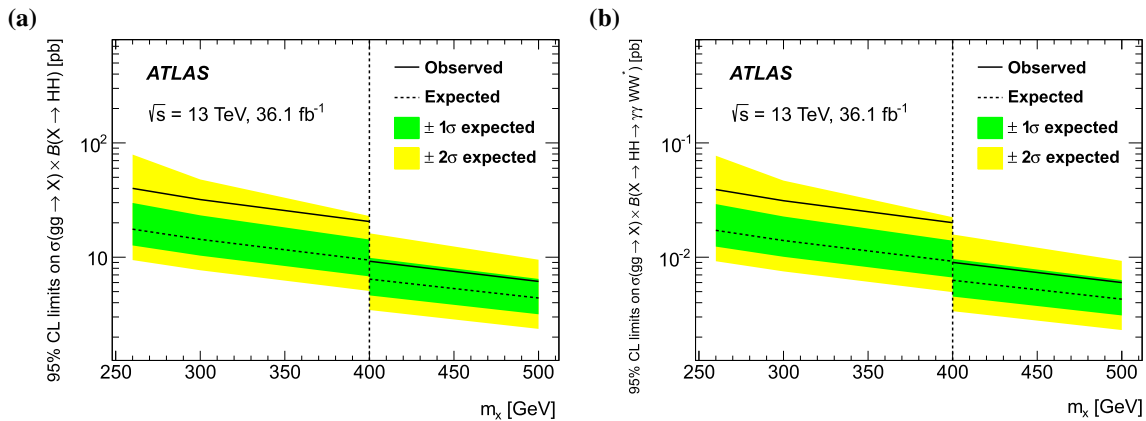


Fig. 4 95% CL expected (dashed line) and observed (solid line) limits on the resonant Higgs boson pair production cross section times the branching fraction of $X \rightarrow HH$ as a function of m_X (a) with and (b) without assuming the SM branching fractions of $H \rightarrow WW^*$ and $H \rightarrow \gamma\gamma$.

The CL_s method and the asymptotic approximation are used. The $\pm 1\sigma$ and $\pm 2\sigma$ bands on the expected limit are also presented. To the right of the vertical dashed line at $m_X = 400$ GeV, the $p_T^{\gamma\gamma} > 100$ GeV selection is applied in both plots, but not to the left

limits, while the impact of systematic uncertainties on these limits is only a few percent.

8 Conclusion

This paper presents searches for non-resonant and resonant Higgs boson pair production with a semileptonic $\gamma\gamma WW^*$ final state using 36.1 fb^{-1} of pp collision data collected at 13 TeV with the ATLAS detector at the LHC. No significant excess above the expected SM background is observed. A 95% confidence-level upper limit of 7.7 pb is set on the cross section for non-resonant production, while the expected limit is 5.4 pb, compared to the SM Higgs boson pair production cross section of 33.4 fb. The observed upper limit on the resonant production cross section times the branching fraction of $X \rightarrow HH$ ranges between 40 pb and 6.1 pb, while the expected limit ranges between 17.6 and 4.4 pb, for a hypothetical resonance with a mass in the range of 260–500 GeV. When deriving the limits above, the SM branching ratios of the $H \rightarrow \gamma\gamma$ and $H \rightarrow WW^*$ are assumed.

Acknowledgements We thank CERN for the very successful operation of the LHC, as well as the support staff from our institutions without whom ATLAS could not be operated efficiently. We acknowledge the support of ANPCyT, Argentina; YerPhI, Armenia; ARC, Australia; BMWFW and FWF, Austria; ANAS, Azerbaijan; SSTC,

Belarus; CNPq and FAPESP, Brazil; NSERC, NRC and CFI, Canada; CERN; CONICYT, Chile; CAS, MOST and NSFC, China; COLCIENCIAS, Colombia; MSMT CR, MPO CR and VSC CR, Czech Republic; DNRF and DNSRC, Denmark; IN2P3-CNRS, CEA-DRF/IRFU, France; SRNSFG, Georgia; BMBF, HGF, and MPG, Germany; GSRT, Greece; RGC, Hong Kong SAR, China; ISF and Benozio Center, Israel; INFN, Italy; MEXT and JSPS, Japan; CNRST, Morocco; NWO, Netherlands; RCN, Norway; MNiSW and NCN, Poland; FCT, Portugal; MNE/IFA, Romania; MES of Russia and NRC KI, Russian Federation; JINR; MESTD, Serbia; MSSR, Slovakia; ARRS and MIZŠ, Slovenia; DST/NRF, South Africa; MINECO, Spain; SRC and Wallenberg Foundation, Sweden; SERI, SNSF and Cantons of Bern and Geneva, Switzerland; MOST, Taiwan; TAEK, Turkey; STFC, United Kingdom; DOE and NSF, United States of America. In addition, individual groups and members have received support from BCKDF, CANARIE, CRC and Compute Canada, Canada; COST, ERC, ERDF, Horizon 2020, and Marie Skłodowska-Curie Actions, European Union; Investissements d'Avenir Labex and Idex, ANR, France; DFG and AvH Foundation, Germany; Herakleitos, Thales and Aristeia programmes co-financed by EU-ESF and the Greek NSRF, Greece; BSF-NSF and GIF, Israel; CERCA Programme Generalitat de Catalunya, Spain; The Royal Society and Leverhulme Trust, United Kingdom. The crucial computing support from all WLCG partners is acknowledged gratefully, in particular from CERN, the ATLAS Tier-1 facilities at TRIUMF (Canada), NDGF (Denmark, Norway, Sweden), CC-IN2P3 (France), KIT/GridKA (Germany), INFN-CNAF (Italy), NL-T1 (Netherlands), PIC (Spain), ASGC (Taiwan), RAL (UK) and BNL (USA), the Tier-2 facilities worldwide and large non-WLCG resource providers. Major contributors of computing resources are listed in Ref. [94].

Open Access This article is distributed under the terms of the Creative Commons Attribution 4.0 International License (<http://creativecommons.org/licenses/by/4.0/>), which permits unrestricted use, distribution, and reproduction in any medium, provided you give appropriate credit to the original author(s) and the source, provide a link to the Creative Commons license, and indicate if changes were made. Funded by SCOAP³.

References

- ATLAS Collaboration, Observation of a new particle in the search for the Standard Model Higgs boson with the ATLAS detector at the LHC. *Phys. Lett. B* **716**, 1 (2012). [arXiv:1207.7214](#) [hep-ex]
- CMS Collaboration, Observation of a new boson at a mass of 125 GeV with the CMS experiment at the LHC. *Phys. Lett. B* **716**, 30 (2012). [arXiv:1207.7235](#) [hep-ex]
- ATLAS Collaboration, Study of the spin and parity of the Higgs boson in diboson decays with the ATLAS detector. *Eur. Phys. J. C* **75**, 476 (2015). [arXiv:1506.05669](#) [hep-ex]
- ATLAS Collaboration, Measurements of the Higgs boson production and decay rates and coupling strengths using pp collision data at $\sqrt{s} = 7$ and 8 TeV in the ATLAS experiment. *Eur. Phys. J. C* **76**, 6 (2016). [arXiv:1507.04548](#) [hep-ex]
- CMS Collaboration, Precise determination of the mass of the Higgs boson and tests of compatibility of its couplings with the standard model predictions using proton collisions at 7 and 8 TeV. *Eur. Phys. J. C* **75**, 212 (2015). [arXiv:1412.8662](#) [hep-ex]
- CMS Collaboration, Constraints on the spin-parity and anomalous HVV couplings of the Higgs boson in proton collisions at 7 and 8 TeV. *Phys. Rev. D* **92**, 012004 (2015). [arXiv:1411.3441](#) [hep-ex]
- ATLAS and CMS Collaborations, Measurements of the Higgs boson production and decay rates and constraints on its couplings from a combined ATLAS and CMS analysis of the LHC pp collision data at $\sqrt{s} = 7$ and 8 TeV. *JHEP* **08**, 045 (2016). [arXiv:1606.02266](#) [hep-ex]
- ATLAS Collaboration, Search for Higgs boson pair production in the $b\bar{b}b\bar{b}$ final state from pp collisions at $\sqrt{s} = 8$ TeV with the ATLAS detector. *Eur. Phys. J. C* **75**, 412 (2015). [arXiv:1506.00285](#) [hep-ex]
- ATLAS Collaboration, Search for Higgs boson pair production in the $\gamma\gamma b\bar{b}$ final state using pp collision data at $\sqrt{s} = 8$ TeV from the ATLAS detector. *Phys. Rev. Lett.* **114**, 081802 (2015). [arXiv:1406.5053](#) [hep-ex]
- CMS Collaboration, Search for two Higgs bosons in final states containing two photons and two bottom quarks in proton–proton collisions at 8 TeV. *Phys. Rev. D* **94**, 052012 (2016). [arXiv:1603.06896](#) [hep-ex]
- ATLAS Collaboration, Searches for Higgs boson pair production in the $hh \rightarrow b\bar{b}\tau\tau$, $\gamma\gamma WW^*$, $\gamma\gamma b\bar{b}$, $b\bar{b}b\bar{b}$ channels with the ATLAS detector. *Phys. Rev. D* **92**, 092004, (2015). [arXiv:1509.04670](#) [hep-ex]
- ATLAS Collaboration, Searches for a heavy scalar boson H decaying to a pair of 125 GeV Higgs bosons hh or for a heavy pseudoscalar boson A decaying to Zh , in the final states with $h \rightarrow \tau\tau$. *Phys. Lett. B* **755**, 217 (2016). [arXiv:1510.01181](#) [hep-ex]
- CMS Collaboration, Search for Higgs boson pair production in the $b\bar{b}\tau\tau$ final state in proton–proton collisions at $\sqrt{s} = 8$ TeV. *Phys. Rev. D* **96**, 072004 (2017). [arXiv:1707.00350](#) [hep-ex]
- CMS Collaboration, Searches for heavy Higgs bosons in two-Higgs-doublet models and for $t \rightarrow ch$ decay using multilepton and diphoton final states in pp collisions at 8 TeV. *Phys. Rev. D* **90**, 112013 (2014). [arXiv:1410.2751](#) [hep-ex]
- ATLAS Collaboration, Search for pair production of Higgs bosons in the $b\bar{b}b\bar{b}$ final state using proton–proton collisions at $\sqrt{s} = 13$ TeV with the ATLAS detector (2018). [arXiv:1804.06174](#) [hep-ex]
- CMS Collaboration, Search for resonant and nonresonant Higgs-boson pair production in the $b\bar{b}\ell\nu\ell\nu$ final state in proton–proton collisions at $\sqrt{s} = 13$ TeV. *JHEP* **01**, 054 (2018). [arXiv:1708.04188](#) [hep-ex]
- LHC Higgs Cross Section Working Group, Handbook of LHC Higgs cross sections: 4. deciphering the nature of the Higgs sector (2016). <https://cds.cern.ch/record/2227475>
- E.W.N. Glover, J.J. van der Bij, Higgs boson pair production via gluon fusion. *Nucl. Phys. B* **309**, 282 (1988)
- J. Baglio et al., The measurement of the Higgs self-coupling at the LHC: theoretical status. *JHEP* **04**, 151 (2013). [arXiv:1212.5581](#) [hep-ph]
- G.C. Branco et al., Theory and phenomenology of two-Higgs-doublet models. *Phys. Rept.* **516**, 1 (2012). [arXiv:1106.0034](#) [hep-ph]
- S. Dimopoulos, H. Georgi, Softly broken supersymmetry and SU(5). *Nucl. Phys. B* **193**, 150 (1981)
- Z. Chacko, Y. Nomura, M. Papucci, G. Perez, Natural little hierarchy from a partially goldstone twin Higgs. *JHEP* **01**, 126 (2006). [arXiv:0510273](#) [hep-ph]
- R. Gröber, M. Mühlleitner, Composite Higgs boson pair production at the LHC. *JHEP* **06**, 020 (2011). [arXiv:1012.1562](#) [hep-ph]
- J. Mrazek et al., The other natural two Higgs doublet model. *Nucl. Phys. B* **853**, 1 (2011). [arXiv:1105.5403](#) [hep-ph]
- Y. Tang, Implications of LHC searches for massive graviton. *JHEP* **08**, 078 (2012). [arXiv:1206.6949](#) [hep-ph]
- K. Cheung, Phenomenology of radion in Randall–Sundrum scenario. *Phys. Rev. D* **63**, 056007 (2001). [arXiv:0009232](#) [hep-ph]
- N. Kumar, S.P. Martin, LHC search for di-Higgs decays of stoponium and other scalars in events with two photons and two bottom jets. *Phys. Rev. D* **90**, 055007 (2014). [arXiv:1404.0996](#) [hep-ph]
- ATLAS Collaboration, The ATLAS experiment at the CERN large-hadron collider. *JINST* **3**, S08003 (2008)
- ATLAS Collaboration, ATLAS insertable B-layer technical design report (2010). <https://cds.cern.ch/record/1291633>
- ATLAS Collaboration, Performance of the ATLAS trigger system in 2015. *Eur. Phys. J. C* **77**, 317 (2017). [arXiv:1611.09661](#) [hep-ex]
- J. Alwall et al., The automated computation of tree-level and next-to-leading order differential cross sections, and their matching to parton shower simulations. *JHEP* **07**, 079 (2014). [arXiv:1405.0301](#) [hep-ph]
- R. Frederix et al., Higgs pair production at the LHC with NLO and parton-shower effects. *Phys. Lett. B* **732**, 142 (2014). [arXiv:1401.7340](#) [hep-ph]
- B. Hespel, D. Lopez-Val, E. Vryonidou, Higgs pair production via gluon fusion in the Two-Higgs-Doublet Model. *JHEP* **09**, 124 (2014). [arXiv:1407.0281](#) [hep-ph]
- S. Frixione, B.R. Webber, Matching NLO QCD computations and parton shower simulations. *JHEP* **06**, 029 (2002). [arXiv:0204244](#) [hep-ph]
- J. Bellm et al., Herwig++ 2.7 Release Note (2013). [arXiv:1310.6877](#) [hep-ph]
- S. Gieseke, C. Rohr, A. Siodmok, Colour reconnections in Herwig++. *Eur. Phys. J. C* **72**, 2225 (2012). [arXiv:1206.0041](#) [hep-ph]
- P.M. Nadolsky et al., Implications of CTEQ global analysis for collider observables. *Phys. Rev. D* **78**, 013004 (2008). [arXiv:0802.0007](#) [hep-ph]
- M. Grazzini et al., Higgs boson pair production at NNLO with top quark mass effects. *JHEP* **05**, 059 (2018). [arXiv:1803.02463](#) [hep-ph]
- S. Borowka et al., Higgs boson pair production in gluon fusion at next-to-leading order with full top-quark mass dependence. *Phys. Rev. Lett.* **117**, 012001 (2016). [arXiv:1604.06447](#) [hep-ph]

40. ATLAS Collaboration, Measurement of the Z/γ^* boson transverse momentum distribution in pp collisions at $\sqrt{s} = 7$ TeV with the ATLAS detector. *JHEP* **09**, 145 (2014). [arXiv:1406.3660](#) [hep-ex]
41. E. Bagnaschi, G. Degrassi, P. Slavich, A. Vicini, Higgs production via gluon fusion in the POWHEG approach in the SM and in the MSSM. *JHEP* **02**, 088 (2012). [arXiv:1111.2854](#) [hep-ph]
42. K. Hamilton, P. Nason, G. Zanderighi, MINLO: Multi-scale improved NLO. *JHEP* **10**, 155 (2012). [arXiv:1206.3572](#) [hep-ph]
43. K. Hamilton, P. Nason, C. Oleari, G. Zanderighi, Merging H/W/Z + 0 and 1 jet at NLO with no merging scale: a path to parton shower + NNLO matching. *JHEP* **05**, 082 (2013). [arXiv:1212.4504](#) [hep-ph]
44. S. Catani, M. Grazzini, Next-to-next-to-leading-order subtraction formalism in Hadron collisions and its application to Higgs–Boson production at the large Hadron collider. *Phys. Rev. Lett.* **98**, 222002 (2007). [arXiv:hep-ph/0703012](#) [hep-ph]
45. M. Grazzini, NNLO predictions for the Higgs boson signal in the $H \rightarrow WW \rightarrow l\nu l\nu$ and $H \rightarrow ZZ \rightarrow 4l$ decay channels. *JHEP* **02**, 043 (2008). [arXiv:0801.3232](#) [hep-ph]
46. M. Grazzini, H. Sargsyan, Heavy-quark mass effects in Higgs boson production at the LHC. *JHEP* **09**, 129 (2013). [arXiv:1306.4581](#) [hep-ph]
47. K. Hamilton, P. Nason, E. Re, G. Zanderighi, NNLOPS simulation of Higgs boson production. *JHEP* **10**, 222 (2013). [arXiv:1309.0017](#) [hep-ph]
48. J. Butterworth et al., PDF4LHC recommendations for LHC Run II. *J. Phys. G* **43**, 023001 (2016). [arXiv:1510.03865](#) [hep-ph]
49. C. Anastasiou et al., High precision determination of the gluon fusion Higgs boson cross-section at the LHC. *JHEP* **05**, 058 (2016). [arXiv:1602.00695](#) [hep-ph]
50. P. Nason, C. Oleari, NLO Higgs boson production via vector-boson fusion matched with shower in POWHEG. *JHEP* **02**, 037 (2010). [arXiv:0911.5299](#) [hep-ph]
51. S. Alioli, P. Nason, C. Oleari, E. Re, A general framework for implementing NLO calculations in shower Monte Carlo programs: the POWHEG BOX. *JHEP* **06**, 043 (2010). [arXiv:1002.2581](#) [hep-ph]
52. M. Ciccolini, A. Denner, S. Dittmaier, Electroweak and QCD corrections to Higgs production via vector-boson fusion at the LHC. *Phys. Rev. D* **77**, 013002 (2008). [arXiv:0710.4749](#) [hep-ph]
53. M. Ciccolini, A. Denner, S. Dittmaier, Strong and electroweak corrections to the production of a Higgs Boson + 2Jets via weak interactions at the large Hadron collider. *Phys. Rev. Lett.* **99**, 161803 (2007). [arXiv:0707.0381](#) [hep-ph]
54. K. Arnold, VBFNLO: A parton level Monte Carlo for processes with electroweak bosons. *Comput. Phys. Commun.* **180**, 1661 (2009). [arXiv:0811.4559](#) [hep-ph]
55. P. Bolzoni, F. Maltoni, S.-O. Moch, M. Zaro, Higgs Boson production via vector-Boson fusion at next-to-next-to-leading order in QCD. *Phys. Rev. Lett.* **105**, 011801 (2010). [arXiv:1003.4451](#) [hep-ph]
56. O. Brein, A. Djouadi, R. Harlander, NNLO QCD corrections to the Higgs-strahlung processes at hadron colliders. *Phys. Lett. B* **579**, 149 (2004). [arXiv:0307206](#) [hep-ph]
57. M.L. Ciccolini, S. Dittmaier, M. Kramer, Electroweak radiative corrections to associated WH and ZH production at hadron colliders. *Phys. Rev. D* **68**, 073003 (2003). [arXiv:0306234](#) [hep-ph]
58. L. Altenkamp, S. Dittmaier, R.V. Harlander, H. Rzehak, T.J.E. Zirke, Gluon-induced Higgs-strahlung at next-to-leading order QCD. *JHEP* **02**, 078 (2013). [arXiv:1211.5015](#) [hep-ph]
59. W. Beenakker, Higgs radiation off top quarks at the tevatron and the LHC. *Phys. Rev. Lett.* **87**, 201805 (2001). [arXiv:0107081](#) [hep-ph]
60. W. Beenakker et al., NLO QCD corrections to $t\bar{t}H$ production in hadron collisions. *Nucl. Phys. B* **653**, 151 (2003). [arXiv:0211352](#) [hep-ph]
61. S. Dawson, L.H. Orr, L. Reina, D. Wackerth, Next-to-leading order QCD corrections to $pp \rightarrow t\bar{t}h$ at the CERN large Hadron collider. *Phys. Rev. D* **67**, 071503 (2003). [arXiv:0211438](#) [hep-ph]
62. S. Dawson, C. Jackson, L.H. Orr, L. Reina, D. Wackerth, Associated Higgs boson production with top quarks at the CERN large Hadron collider: NLO QCD corrections. *Phys. Rev. D* **68**, 034022 (2003). [arXiv:0305087](#) [hep-ph]
63. ATLAS Collaboration, Summary of ATLAS Pythia 8 tunes, ATL-PHYS-PUB-2012-003 (2012). <https://cds.cern.ch/record/1474107>
64. A.D. Martin, W.J. Stirling, R.S. Thorne, G. Watt, Parton distributions for the LHC. *Eur. Phys. J. C* **63**, 189 (2009). [arXiv:0901.0002](#) [hep-ph]
65. S. Agostinelli, GEANT4—A simulation toolkit. *Nucl. Instrum. Methods A* **506**, 250 (2003)
66. ATLAS Collaboration, The ATLAS simulation infrastructure. *Eur. Phys. J. C* **70**, 823 (2010). [arXiv:1005.4568](#) [hep-ex]
67. ATLAS Collaboration, Electron and photon energy calibration with the ATLAS detector using data collected in 2015 at $\sqrt{s} = 13$ TeV, ATL-PHYS-PUB-2016-015 (2016). <https://cds.cern.ch/record/2203514>
68. ATLAS Collaboration, Measurement of the photon identification efficiencies with the ATLAS detector using LHC Run-1 data. *Eur. Phys. J. C* **76**, 666 (2016). [arXiv:1606.01813](#) [hep-ex]
69. ATLAS Collaboration, Electron and photon energy calibration with the ATLAS detector using LHC Run 1 data. *Eur. Phys. J. C* **74**, 3071 (2014). [arXiv:1407.5063](#) [hep-ex]
70. ATLAS Collaboration, Measurement of the inclusive isolated prompt photon cross section in pp collisions at $\sqrt{s} = 7$ TeV with the ATLAS detector. *Phys. Rev. D* **83**, 052005 (2011). [arXiv:1012.4389](#) [hep-ex]
71. ATLAS Collaboration, Topological cell clustering in the ATLAS calorimeters and its performance in LHC Run 1. *Eur. Phys. J. C* **77**, 490 (2017). [arXiv:1603.02934](#) [hep-ex]
72. ATLAS Collaboration, Electron efficiency measurements with the ATLAS detector using the 2015 LHC proton-proton collision data, ATLAS-CONF-2016-024 (2016). <https://cds.cern.ch/record/2157687>
73. ATLAS Collaboration, Muon reconstruction performance of the ATLAS detector in proton–proton collision data at $\sqrt{s} = 13$ TeV. *Eur. Phys. J. C* **76**, 292 (2016). [arXiv:1603.05598](#) [hep-ex]
74. M. Cacciari, G.P. Salam, G. Soyez, FastJet user manual. *Eur. Phys. J. C* **72**, 1896 (2012). [arXiv:1111.6097](#) [hep-ph]
75. M. Cacciari, G.P. Salam, G. Soyez, The anti- k_r jet clustering algorithm. *JHEP* **04**, 063 (2008). [arXiv:0802.1189](#) [hep-ph]
76. ATLAS Collaboration, Jet energy measurement with the ATLAS detector in proton–proton collisions at $\sqrt{s} = 7$ TeV. *Eur. Phys. J. C* **73**, 2304 (2013). [arXiv:1112.6426](#) [hep-ex]
77. ATLAS Collaboration, Jet energy measurement and its systematic uncertainty in proton–proton collisions at $\sqrt{s} = 7$ TeV with the ATLAS detector. *Eur. Phys. J. C* **75**, 17 (2015). [arXiv:1406.0076](#) [hep-ex]
78. ATLAS Collaboration, Jet energy resolution in proton–proton collisions at $\sqrt{s} = 7$ TeV recorded in 2010 with the ATLAS detector. *Eur. Phys. J. C* **73**, 2306 (2013). [arXiv:1210.6210](#) [hep-ex]
79. ATLAS Collaboration, Performance of pile-up mitigation techniques for jets in pp collisions at $\sqrt{s} = 8$ TeV using the ATLAS detector. *Eur. Phys. J. C* **76**, 581 (2016). [arXiv:1510.03823](#) [hep-ex]
80. ATLAS Collaboration, Jet Calibration and systematic uncertainties for jets reconstructed in the ATLAS detector at $\sqrt{s} = 13$ TeV, ATL-PHYS-PUB-2015-015 (2015). <https://cds.cern.ch/record/2037613>
81. ATLAS Collaboration, Tagging and suppression of pileup jets, ATL-PHYS-PUB-2014-001 (2014). <https://atlas.web.cern.ch/Atlas/GROUPS/PHYSICS/PUBNOTES/ATL-PHYS-PUB-2014-001/>

82. ATLAS Collaboration, Performance of b -jet identification in the ATLAS experiment, JINST 11 P04008 (2016). [arXiv:1512.01094](https://arxiv.org/abs/1512.01094) [hep-ex]
83. ATLAS Collaboration, Expected performance of the ATLAS b -tagging algorithms in Run-2, ATL-PHYS-PUB-2015-022 (2015). <https://cds.cern.ch/record/2037697>
84. ATLAS Collaboration, Performance of missing transverse momentum reconstruction for the ATLAS detector in the first proton–proton collisions at $\sqrt{s} = 13$ TeV, ATL-PHYS-PUB-2015-027 (2015). <https://cds.cern.ch/record/2037904>
85. ATLAS Collaboration, Expected performance of missing transverse momentum reconstruction for the ATLAS detector at $\sqrt{s} = 13$ TeV, ATL-PHYS-PUB-2015-023 (2015). <https://cds.cern.ch/record/2037700>
86. M. Oreglia, A study of the reactions $\psi' \rightarrow \gamma\gamma\psi$ (1980). <https://www.slac.stanford.edu/cgi-wrap/getdoc/slac-r-236.pdf>
87. ATLAS Collaboration, Combined measurement of the Higgs Boson mass in pp collisions at $\sqrt{s} = 7$ and 8 TeV with the ATLAS and CMS experiments. Phys. Rev. Lett. **114**, 191803 (2015). [arXiv:1503.07589](https://arxiv.org/abs/1503.07589) [hep-ex]
88. ATLAS Collaboration, Luminosity determination in pp collision-sat $\sqrt{s} = 8$ TeV using the ATLAS detector at the LHC. Eur. Phys. J. C **76**, 653 (2016). [arXiv:1608.03953](https://arxiv.org/abs/1608.03953) [hep-ex]
89. ATLAS Collaboration, Performance of the ATLAS trigger system in 2010. Eur. Phys. J. C **72**, 1849 (2012). [arXiv:1110.1530](https://arxiv.org/abs/1110.1530) [hep-ex]
90. ATLAS Collaboration, Jet energy scale measurements and their systematic uncertainties in proton–proton collisions at $\sqrt{s} = 13$ TeV with the ATLAS detector. Phys. Rev. D **96**, 072002 (2017). [arXiv:1703.09665](https://arxiv.org/abs/1703.09665) [hep-ex]
91. ATLAS Collaboration, Properties of Jets and inputs to jet reconstruction and calibration with the ATLAS detector using Proton–Proton collisions at $\sqrt{s} = 13$ TeV, ATL-PHYS-PUB-2015-036 (2015). <https://cds.cern.ch/record/2044564>
92. G. Cowan et al., Asymptotic formulae for likelihood-based tests of new physics. Eur. Phys. J. C **71**, 1554 (2011). [arXiv:1007.1727](https://arxiv.org/abs/1007.1727) [physics.data-an]
93. A.L. Read, Presentation of search results: the CL_s technique. J. Phys. G **28**, 2693 (2002)
94. ATLAS Collaboration, ATLAS Computing Acknowledgements, ATL-GEN-PUB-2016-002. <https://cds.cern.ch/record/2202407>

ATLAS Collaboration

M. Aaboud^{34d}, G. Aad⁹⁹, B. Abbott¹²⁵, O. Abdinov^{13,*}, B. Abeloos¹²⁹, D. K. Abhayasinghe⁹¹, S. H. Abidi¹⁶⁴, O. S. AbouZeid¹⁴³, N. L. Abraham¹⁵³, H. Abramowicz¹⁵⁸, H. Abreu¹⁵⁷, Y. Abulaiti⁶, B. S. Acharya^{64a,64b,p}, S. Adachi¹⁶⁰, L. Adamczyk^{81a}, J. Adelman¹¹⁹, M. Adersberger¹¹², A. Adiguzel^{12c,aj}, T. Adye¹⁴¹, A. A. Affolder¹⁴³, Y. Afik¹⁵⁷, C. Agheorghiesei^{27c}, J. A. Aguilar-Saavedra^{137a,137f}, F. Ahmadov^{77,ah}, G. Aielli^{71a,71b}, S. Akatsuka⁸³, T. P. A. Åkesson⁹⁴, E. Akilli⁵², A. V. Akimov¹⁰⁸, G. L. Alberghi^{23a,23b}, J. Albert¹⁷³, P. Albicocco⁴⁹, M. J. Alconada Verzini⁸⁶, S. Alderweireldt¹¹⁷, M. Aleksa³⁵, I. N. Aleksandrov⁷⁷, C. Alexa^{27b}, G. Alexander¹⁵⁸, T. Alexopoulos¹⁰, M. Alhroob¹²⁵, B. Ali¹³⁹, G. Alimonti^{66a}, J. Alison³⁶, S. P. Alkire¹⁴⁵, C. Allaire¹²⁹, B. M. M. Allbrooke¹⁵³, B. W. Allen¹²⁸, P. P. Allport²¹, A. Aloisio^{67a,67b}, A. Alonso³⁹, F. Alonso⁸⁶, C. Alpigiani¹⁴⁵, A. A. Alshehri⁵⁵, M. I. Alstary⁹⁹, B. Alvarez Gonzalez³⁵, D. Álvarez Piqueras¹⁷¹, M. G. Alvigi^{67a,67b}, B. T. Amadio¹⁸, Y. Amaral Coutinho^{78b}, L. Ambroz¹³², C. Amelung²⁶, D. Amidei¹⁰³, S. P. Amor Dos Santos^{137a,137c}, S. Amoroso³⁵, C. S. Amrouche⁵², C. Anastopoulos¹⁴⁶, L. S. Ancu⁵², N. Andari²¹, T. Andeen¹¹, C. F. Anders^{59b}, J. K. Anders²⁰, K. J. Anderson³⁶, A. Andreazza^{66a,66b}, V. Andrei^{59a}, C. R. Anelli¹⁷³, S. Angelidakis³⁷, I. Angelozzi¹¹⁸, A. Angerami³⁸, A. V. Anisenkov^{120a,120b}, A. Annovi^{69a}, C. Antel^{59a}, M. T. Anthony¹⁴⁶, M. Antonelli⁴⁹, D. J. A. Antrim¹⁶⁸, F. Anulli^{70a}, M. Aoki⁷⁹, L. Aperio Bella³⁵, G. Arabidze¹⁰⁴, Y. Arai⁷⁹, J. P. Araque^{137a}, V. Araujo Ferraz^{78b}, R. Araujo Pereira^{78b}, A. T. H. Arce⁴⁷, R. E. Ardell⁹¹, F. A. Arduh⁸⁶, J-F. Arguin¹⁰⁷, S. Argyropoulos⁷⁵, A. J. Armbruster³⁵, L. J. Armitage⁹⁰, A. Armstrong¹⁶⁸, O. Arnaez¹⁶⁴, H. Arnold¹¹⁸, M. Arratia³¹, O. Arslan²⁴, A. Artamonov^{109,*}, G. Artoni¹³², S. Artz⁹⁷, S. Asai¹⁶⁰, N. Asbah⁴⁴, A. Ashkenazi¹⁵⁸, E. M. Asimakopoulou¹⁶⁹, L. Asquith¹⁵³, K. Assamagan²⁹, R. Astalos^{28a}, R. J. Atkin^{32a}, M. Atkinson¹⁷⁰, N. B. Atlay¹⁴⁸, K. Augsten¹³⁹, G. Avolio³⁵, R. Avramidou^{58a}, B. Axen¹⁸, M. K. Ayoub^{15a}, G. Azuelos^{107,aw}, A. E. Baas^{59a}, M. J. Baca²¹, H. Bachacou¹⁴², K. Bachas^{65a,65b}, M. Backes¹³², P. Bagnaia^{70a,70b}, M. Bahmani⁸², H. Bahrasemani¹⁴⁹, A. J. Bailey¹⁷¹, J. T. Baines¹⁴¹, M. Bajic³⁹, C. Bakalis¹⁰, O. K. Baker¹⁸⁰, P. J. Bakker¹¹⁸, D. Bakshi Gupta⁹³, E. M. Baldin^{120a,120b}, P. Balek¹⁷⁷, F. Balli¹⁴², W. K. Balunas¹³⁴, J. Balz⁹⁷, E. Banas⁸², A. Bandyopadhyay²⁴, S. Banerjee^{178,1}, A. A. E. Bannoura¹⁷⁹, L. Barak¹⁵⁸, W. M. Barbe³⁷, E. L. Barberio¹⁰², D. Barberis^{53a,53b}, M. Barbero⁹⁹, T. Barillari¹¹³, M-S. Barisits³⁵, J. Barkeloo¹²⁸, T. Barklow¹⁵⁰, N. Barlow³¹, R. Barnea¹⁵⁷, S. L. Barnes^{58c}, B. M. Barnett¹⁴¹, R. M. Barnett¹⁸, Z. Barnovska-Blenessy^{58a}, A. Baroncelli^{72a}, G. Barone²⁶, A. J. Barr¹³², L. Barranco Navarro¹⁷¹, F. Barreiro⁹⁶, J. Barreiro Guimarães da Costa^{15a}, R. Bartoldus¹⁵⁰, A. E. Barton⁸⁷, P. Bartos^{28a}, A. Basalae¹³⁵, A. Bassalat¹²⁹, R. L. Bates⁵⁵, S. J. Batista¹⁶⁴, S. Batlamous^{34e}, J. R. Batley³¹, M. Battaglia¹⁴³, M. Bauce^{70a,70b}, F. Bauer¹⁴², K. T. Bauer¹⁶⁸, H. S. Bawa^{150,n}, J. B. Beacham¹²³, M. D. Beattie⁸⁷, T. Beau¹³³, P. H. Beauchemin¹⁶⁷, P. Bechtel²⁴, H. C. Beck⁵¹, H. P. Beck^{20,t}, K. Becker⁵⁰, M. Becker⁹⁷, C. Becot⁴⁴, A. Beddall^{12d}, A. J. Beddall^{12a}, V. A. Bednyakov⁷⁷, M. Bedognetti¹¹⁸, C. P. Bee¹⁵², T. A. Beermann³⁵, M. Begalli^{78b}, M. Begel²⁹, A. Behera¹⁵², J. K. Behr⁴⁴, A. S. Bell⁹², G. Bella¹⁵⁸, L. Bellagamba^{23b}, A. Bellerive³³, M. Bellomo¹⁵⁷, P. Bellos⁹, K. Belotskiy¹¹⁰, N. L. Belyaev¹¹⁰, O. Benary^{158,*}, D. Benchekroun^{34a}, M. Bender¹¹², N. Benekos¹⁰, Y. Benhammou¹⁵⁸, E. Benhar Nocchioli¹⁸⁰, J. Benitez⁷⁵, D. P. Benjamin⁴⁷, M. Benoit⁵², J. R. Bensinger²⁶, S. Bentvelsen¹¹⁸, L. Beresford¹³², M. Beretta⁴⁹, D. Berge⁴⁴, E. Bergeas Kuutmann¹⁶⁹, N. Berger⁵,

L. J. Bergsten²⁶, J. Beringer¹⁸, S. Berlendis⁷, N. R. Bernard¹⁰⁰, G. Bernardi¹³³, C. Bernius¹⁵⁰, F. U. Bernlochner²⁴, T. Berry⁹¹, P. Berta⁹⁷, C. Bertella^{15a}, G. Bertoli^{43a,43b}, I. A. Bertram⁸⁷, G. J. Besjes³⁹, O. Bessidskaia Bylund^{43a,43b}, M. Bessner⁴⁴, N. Besson¹⁴², A. Bethani⁹⁸, S. Bethke¹¹³, A. Betti²⁴, A. J. Bevan⁹⁰, J. Beyer¹¹³, R. M. Bianchi¹³⁶, O. Biebel¹¹², D. Biedermann¹⁹, R. Bielski⁹⁸, K. Bierwagen⁹⁷, N. V. Biesuz^{69a,69b}, M. Biglietti^{72a}, T. R. V. Billoud¹⁰⁷, M. Bindi⁵¹, A. Bingul^{12d}, C. Bini^{70a,70b}, S. Biondi^{23a,23b}, T. Bisanz⁵¹, J. P. Biswal¹⁵⁸, C. Bittrich⁴⁶, D. M. Bjergaard⁴⁷, J. E. Black¹⁵⁰, K. M. Black²⁵, R. E. Blair⁶, T. Blazek^{28a}, I. Bloch⁴⁴, C. Blocker²⁶, A. Blue⁵⁵, U. Blumenschein⁹⁰, Dr. Blunier^{144a}, G. J. Bobbink¹¹⁸, V. S. Bobrovnikov^{120a,120b}, S. S. Bocchetta⁹⁴, A. Bocci⁴⁷, D. Boerner¹⁷⁹, D. Bogavac¹¹², A. G. Bogdanchikov^{120a,120b}, C. Bohm^{43a}, V. Boisvert⁹¹, P. Bokan¹⁶⁹, T. Bold^{81a}, A. S. Boldyrev¹¹¹, A. E. Bolz^{59b}, M. Bomben¹³³, M. Bona⁹⁰, J. S. Bonilla¹²⁸, M. Boonekamp¹⁴², A. Borisov¹²¹, G. Borissov⁸⁷, J. Bortfeldt³⁵, D. Bortoletto¹³², V. Bortolotto^{61b,61c,71a,71b}, D. Boscherini^{23b}, M. Bosman¹⁴, J. D. Bossio Sola³⁰, K. Bouaouda^{34a}, J. Boudreau¹³⁶, E. V. Bouhova-Thacker⁸⁷, D. Boumediene³⁷, C. Bourdarios¹²⁹, S. K. Boutle⁵⁵, A. Boveia¹²³, J. Boyd³⁵, I. R. Boyko⁷⁷, A. J. Bozson⁹¹, J. Bracik²¹, N. Brahim⁹⁹, A. Brandt⁸, G. Brandt¹⁷⁹, O. Brandt^{59a}, F. Braren⁴⁴, U. Bratzler¹⁶¹, B. Brau¹⁰⁰, J. E. Brau¹²⁸, W. D. Breaden Madden⁵⁵, K. Brendlinger⁴⁴, A. J. Brennan¹⁰², L. Brenner⁴⁴, R. Brenner¹⁶⁹, S. Bressler¹⁷⁷, B. Brickwedde⁹⁷, D. L. Briglin²¹, D. Britton⁵⁵, D. Britzger^{59b}, I. Brock²⁴, R. Brock¹⁰⁴, G. Brooijmans³⁸, T. Brooks⁹¹, W. K. Brooks^{144b}, E. Brost¹¹⁹, J. H. Broughton²¹, P. A. Bruckman de Renstrom⁸², D. Bruncko^{28b}, A. Bruni^{23b}, G. Bruni^{23b}, L. S. Bruni¹¹⁸, S. Bruno^{71a,71b}, B.H. Brunt³¹, M. Bruschi^{23b}, N. Brusino¹³⁶, P. Bryant³⁶, L. Bryngemark⁴⁴, T. Buanes¹⁷, Q. Buat³⁵, P. Buchholz¹⁴⁸, A. G. Buckley⁵⁵, I. A. Budagov⁷⁷, M. K. Bugge¹³¹, F. Bühner⁵⁰, O. Bulekov¹¹⁰, D. Bullock⁸, T. J. Burch¹¹⁹, S. Burdin⁸⁸, C. D. Burgard¹¹⁸, A. M. Burger⁵, B. Burghgrave¹¹⁹, K. Burka⁸², S. Burke¹⁴¹, I. Burmeister⁴⁵, J. T. P. Burr¹³², D. Büscher⁵⁰, V. Büscher⁹⁷, E. Buschmann⁵¹, P. Bussey⁵⁵, J. M. Butler²⁵, C. M. Buttar⁵⁵, J. M. Butterworth⁹², P. Butti³⁵, W. Buttinger³⁵, A. Buzatu¹⁵⁵, A. R. Buzykaev^{120a,120b}, G. Cabras^{23a,23b}, S. Cabrera Urbán¹⁷¹, D. Caforio¹³⁹, H. Cai¹⁷⁰, V. M. M. Cairo², O. Cakir^{4a}, N. Calace⁵², P. Calafiura¹⁸, A. Calandri⁹⁹, G. Calderini¹³³, P. Calfayan⁶³, G. Callea^{40a,40b}, L. P. Caloba^{78b}, S. Calvente Lopez⁹⁶, D. Calvet³⁷, S. Calvet³⁷, T. P. Calvet¹⁵², M. Calvetti^{69a,69b}, R. Camacho Toro¹³³, S. Camarda³⁵, P. Camarri^{71a,71b}, D. Cameron¹³¹, R. Caminal Armadans¹⁰⁰, C. Camincher³⁵, S. Campana³⁵, M. Campanelli⁹², A. Camplani³⁹, A. Campoverde¹⁴⁸, V. Canale^{67a,67b}, M. Cano Bret^{58c}, J. Cantero¹²⁶, T. Cao¹⁵⁸, Y. Cao¹⁷⁰, M. D. M. Capeans Garrido³⁵, I. Caprini^{27b}, M. Caprini^{27b}, M. Capua^{40a,40b}, R. M. Carbone³⁸, R. Cardarelli^{71a}, F. C. Cardillo⁵⁰, I. Carli¹⁴⁰, T. Carli³⁵, G. Carlino^{67a}, B. T. Carlson¹³⁶, L. Carminati^{66a,66b}, R. M. D. Carney^{43a,43b}, S. Caron¹¹⁷, E. Carquin^{144b}, S. Carrá^{66a,66b}, G. D. Carrillo-Montoya³⁵, D. Casadei^{32b}, M. P. Casado^{14,h}, A. F. Casha¹⁶⁴, M. Casolino¹⁴, D. W. Casper¹⁶⁸, R. Castelijm¹¹⁸, F. L. Castillo¹⁷¹, V. Castillo Gimenez¹⁷¹, N. F. Castro^{137a,137e}, A. Catinaccio³⁵, J. R. Catmore¹³¹, A. Cattai³⁵, J. Caudron²⁴, V. Cavaliere²⁹, E. Cavallaro¹⁴, D. Cavalli^{66a}, M. Cavalli-Sforza¹⁴, V. Cavasinni^{69a,69b}, E. Celebi^{12b}, F. Ceradini^{72a,72b}, L. Cerda Alberich¹⁷¹, A. S. Cerqueira^{78a}, A. Cerri¹⁵³, L. Cerrito^{71a,71b}, F. Cerutti¹⁸, A. Cervelli^{23a,23b}, S. A. Cetin^{12b}, A. Chafaq^{34a}, D. Chakraborty¹¹⁹, S. K. Chan⁵⁷, W. S. Chan¹¹⁸, Y. L. Chan^{61a}, P. Chang¹⁷⁰, J. D. Chapman³¹, D. G. Charlton²¹, C. C. Chau³³, C. A. Chavez Barajas¹⁵³, S. Che¹²³, A. Chegwidan¹⁰⁴, S. Chekanov⁶, S. V. Chekulaev^{165a}, G. A. Chelkov^{77,av}, M. A. Chelstowska³⁵, C. Chen^{58a}, C. H. Chen⁷⁶, H. Chen²⁹, J. Chen^{58a}, J. Chen³⁸, S. Chen¹³⁴, S. J. Chen^{15c}, X. Chen^{15b,au}, Y. Chen⁸⁰, Y-H. Chen⁴⁴, H. C. Cheng¹⁰³, H. J. Cheng^{15d}, A. Cheplakov⁷⁷, E. Cheremushkina¹²¹, R. Cherkaoui El Moursli^{34e}, E. Cheu⁷, K. Cheung⁶², L. Chevalier¹⁴², V. Chiarella⁴⁹, G. Chiarelli^{69a}, G. Chiodini^{65a}, A. S. Chisholm³⁵, A. Chitan^{27b}, I. Chiu¹⁶⁰, Y. H. Chiu¹⁷³, M. V. Chizhov⁷⁷, K. Choi⁶³, A. R. Chomont¹²⁹, S. Chouridou¹⁵⁹, Y. S. Chow¹¹⁸, V. Christodoulou⁹², M. C. Chu^{61a}, J. Chudoba¹³⁸, A. J. Chuinard¹⁰¹, J. J. Chwastowski⁸², L. Chytka¹²⁷, D. Cinca⁴⁵, V. Cindro⁸⁹, I. A. Cioară²⁴, A. Ciochio¹⁸, F. Ciotto^{67a,67b}, Z. H. Citron¹⁷⁷, M. Citterio^{66a}, A. Clark⁵², M. R. Clark³⁸, P. J. Clark⁴⁸, C. Clement^{43a,43b}, Y. Coadou⁹⁹, M. Cobl^{64a,64c}, A. Coccaro^{53a,53b}, J. Cochran⁷⁶, A. E. C. Coimbra¹⁷⁷, L. Colasurdo¹¹⁷, B. Cole³⁸, A. P. Colijn¹¹⁸, J. Collot⁵⁶, P. Conde Muiño^{137a,137b}, E. Coniavitis⁵⁰, S. H. Connell^{32b}, I. A. Connelly⁹⁸, S. Constantinescu^{27b}, F. Conventi^{67a,ax}, A. M. Cooper-Sarkar¹³², F. Cormier¹⁷², K. J. R. Cormier¹⁶⁴, M. Corradi^{70a,70b}, E. E. Corrigan⁹⁴, F. Corriveau^{101,af}, A. Cortes-Gonzalez³⁵, M. J. Costa¹⁷¹, D. Costanzo¹⁴⁶, G. Cottin³¹, G. Cowan⁹¹, B. E. Cox⁹⁸, J. Crane⁹⁸, K. Cranmer¹²², S. J. Crawley⁵⁵, R. A. Creager¹³⁴, G. Cree³³, S. Crépe-Renaudin⁵⁶, F. Crescioli¹³³, M. Cristinziani²⁴, V. Croft¹²², G. Crosetti^{40a,40b}, A. Cueto⁹⁶, T. Cuhadar Donszelmann¹⁴⁶, A. R. Cukierman¹⁵⁰, M. Curatolo⁴⁹, J. Cúth⁹⁷, S. Czekierda⁸², P. Czodrowski³⁵, M. J. Da Cunha Sargedas De Sousa^{58b}, C. Da Via⁹⁸, W. Dabrowski^{81a}, T. Dado^{28a,aa}, S. Dahbi^{34e}, T. Dai¹⁰³, F. Dallaire¹⁰⁷, C. Dallapiccola¹⁰⁰, M. Dam³⁹, G. D'amen^{23a,23b}, J. Damp⁹⁷, J. R. Dandoy¹³⁴, M. F. Daneri³⁰, N. P. Dang^{178,1}, N. D. Dann⁹⁸, M. Danninger¹⁷², V. Dao³⁵, G. Darbo^{53b}, S. Darmora⁸, O. Dartsis⁵, A. Dattagupta¹²⁸, T. Daubney⁴⁴, S. D'Auria⁵⁵, W. Davey²⁴, C. David⁴⁴, T. Davidek¹⁴⁰, D. R. Davis⁴⁷, E. Dawe¹⁰², I. Dawson¹⁴⁶, K. De⁸, R. De Asmundis^{67a}, A. De Benedetti¹²⁵, S. De Castro^{23a,23b}, S. De Cecco^{70a,70b}, N. De Groot¹¹⁷, P. de Jong¹¹⁸, H. De la Torre¹⁰⁴, F. De Lorenzi⁷⁶, A. De Maria^{51,v}, D. De Pedis^{70a}, A. De Salvo^{70a}, U. De Sanctis^{71a,71b}, A. De Santo¹⁵³, K. De Vasconcelos Corga⁹⁹, J. B. De Vivie De Regie¹²⁹, C. Debenedetti¹⁴³, D. V. Dedovich⁷⁷, N. Dehghanian³

M. Del Gaudio^{40a,40b}, J. Del Peso⁹⁶, D. Delgove¹²⁹, F. Deliot¹⁴², C. M. Delitzsch⁷, M. Della Pietra^{67a,67b}, D. Della Volpe⁵², A. Dell'Acqua³⁵, L. Dell'Asta²⁵, M. Delmastro⁵, C. Delporte¹²⁹, P. A. Delsart⁵⁶, D. A. DeMarco¹⁶⁴, S. Demers¹⁸⁰, M. Demichev⁷⁷, S. P. Denisov¹²¹, D. Denysiuk¹¹⁸, L. D'Eramo¹³³, D. Derendarz⁸², J. E. Derkaoui^{34d}, F. Derue¹³³, P. Dervan⁸⁸, K. Desch²⁴, C. Deterre⁴⁴, K. Dette¹⁶⁴, M. R. Devesa³⁰, P. O. Deviveiros³⁵, A. Dewhurst¹⁴¹, S. Dhaliwal²⁶, F. A. Di Bello⁵², A. Di Ciaccio^{71a,71b}, L. Di Ciaccio⁵, W. K. Di Clemente¹³⁴, C. Di Donato^{67a,67b}, A. Di Girolamo³⁵, B. Di Micco^{72a,72b}, R. Di Nardo³⁵, K. F. Di Petrillo⁵⁷, A. Di Simone⁵⁰, R. Di Sipio¹⁶⁴, D. Di Valentino³³, C. Diaconu⁹⁹, M. Diamond¹⁶⁴, F. A. Dias³⁹, T. Dias Do Vale^{137a}, M. A. Diaz^{144a}, J. Dickinson¹⁸, E. B. Diehl¹⁰³, J. Dietrich¹⁹, S. Díez Cornell⁴⁴, A. Dimitrievska¹⁸, J. Dingfelder²⁴, F. Dittus³⁵, F. Djama⁹⁹, T. Djobava^{156b}, J. I. Djuvsland^{59a}, M. A. B. Do Vale^{78c}, M. Dobre^{27b}, D. Dodsworth²⁶, C. Doglioni⁹⁴, J. Dolejsi¹⁴⁰, Z. Dolezal¹⁴⁰, M. Donadelli^{78d}, J. Donini³⁷, A. D'onofrio⁹⁰, M. D'Onofrio⁸⁸, J. Dopke¹⁴¹, A. Doria^{67a}, M. T. Dova⁸⁶, A. T. Doyle⁵⁵, E. Drechsler⁵¹, E. Dreyer¹⁴⁹, T. Dreyer⁵¹, M. Dris¹⁰, Y. Du^{58b}, J. Duarte-Campderros¹⁵⁸, F. Dubinin¹⁰⁸, A. Dubreuil⁵², E. Duchovni¹⁷⁷, G. Duckeck¹¹², A. Ducourthial¹³³, O. A. Ducu^{107,z}, D. Duda¹¹³, A. Dudarev³⁵, A. C. Dudder⁹⁷, E. M. Duffield¹⁸, L. Dufлот¹²⁹, M. Dührssen³⁵, C. Dülsen¹⁷⁹, M. Dumancic¹⁷⁷, A. E. Dumitriu^{27b,f}, A. K. Duncan⁵⁵, M. Dunford^{59a}, A. Duperrin⁹⁹, H. Duran Yildiz^{4a}, M. Düren⁵⁴, A. Durglishvili^{156b}, D. Duschinger⁴⁶, B. Dutta⁴⁴, D. Duvnjak¹, M. Dyndal⁴⁴, S. Dysch⁹⁸, B. S. Dziedzic⁸², C. Eckardt⁴⁴, K. M. Ecker¹¹³, R. C. Edgar¹⁰³, T. Eifert³⁵, G. Eigen¹⁷, K. Einsweiler¹⁸, T. Ekelof¹⁶⁹, M. El Kacimi^{34c}, R. El Kosseifi⁹⁹, V. Ellajosyula⁹⁹, M. Ellert¹⁶⁹, F. Ellinghaus¹⁷⁹, A. A. Elliot⁹⁰, N. Ellis³⁵, J. Elmsheuser²⁹, M. Elsing³⁵, D. Emelianov¹⁴¹, Y. Enari¹⁶⁰, J. S. Ennis¹⁷⁵, M. B. Epland⁴⁷, J. Erdmann⁴⁵, A. Ereditato²⁰, S. Errede¹⁷⁰, M. Escalier¹²⁹, C. Escobar¹⁷¹, B. Esposito⁴⁹, O. Estrada Pastor¹⁷¹, A. I. Etiennevire¹⁴², E. Etzion¹⁵⁸, H. Evans⁶³, A. Ezhilov¹³⁵, M. Ezzi^{34e}, F. Fabbri⁵⁵, L. Fabbri^{23a,23b}, V. Fabiani¹¹⁷, G. Facini⁹², R. M. Faisca Rodrigues Pereira^{137a}, R. M. Fakhruddinov¹²¹, S. Falciano^{70a}, P. J. Falke⁵, S. Falke⁵, J. Faltova¹⁴⁰, Y. Fang^{15a}, M. Fanti^{66a,66b}, A. Farbin⁸, A. Farilla^{72a}, E. M. Farina^{68a,68b}, T. Farooque¹⁰⁴, S. Farrell¹⁸, S. M. Farrington¹⁷⁵, P. Farthouat³⁵, F. Fassi^{34e}, P. Fassnacht³⁵, D. Fassouliotis⁹, M. Fauci Giannelli⁴⁸, A. Favareto^{53a,53b}, W. J. Fawcett⁵², L. Fayard¹²⁹, O. L. Fedin^{135,r}, W. Fedorko¹⁷², M. Feickert⁴¹, S. Feigl¹³¹, L. Feligioni⁹⁹, C. Feng^{58b}, E. J. Feng³⁵, M. Feng⁴⁷, M. J. Fenton⁵⁵, A. B. Fenyuk¹²¹, L. Feremenga⁸, J. Ferrando⁴⁴, A. Ferrari¹⁶⁹, P. Ferrari¹¹⁸, R. Ferrari^{68a}, D. E. Ferreira de Lima^{59b}, A. Ferrer¹⁷¹, D. Ferrere⁵², C. Ferretti¹⁰³, F. Fiedler⁹⁷, A. Filipčić⁸⁹, F. Filthaut¹¹⁷, K. D. Finelli²⁵, M. C. N. Fiolhais^{137a,137c,b}, L. Fiorini¹⁷¹, C. Fischer¹⁴, W. C. Fisher¹⁰⁴, N. Flaschel⁴⁴, I. Fleck¹⁴⁸, P. Fleischmann¹⁰³, R. R. M. Fletcher¹³⁴, T. Flick¹⁷⁹, B. M. Flierl¹¹², L. M. Flores¹³⁴, L. R. Flores Castillo^{61a}, N. Fomin¹⁷, G. T. Forcolin⁹⁸, A. Formica¹⁴², F. A. Förster¹⁴, A. C. Forti⁹⁸, A. G. Foster²¹, D. Fournier¹²⁹, H. Fox⁸⁷, S. Fracchia¹⁴⁶, P. Francavilla^{69a,69b}, M. Franchini^{23a,23b}, S. Franchino^{59a}, D. Francis³⁵, L. Franconi¹³¹, M. Franklin⁵⁷, M. Frate¹⁶⁸, M. Fraternali^{68a,68b}, D. Freeborn⁹², S. M. Fressard-Batraneanu³⁵, B. Freund¹⁰⁷, W. S. Freund^{78b}, D. Froidevaux³⁵, J. A. Frost¹³², C. Fukunaga¹⁶¹, T. Fusayasu¹¹⁴, J. Fuster¹⁷¹, O. Gabizon¹⁵⁷, A. Gabrielli^{23a,23b}, A. Gabrielli¹⁸, G. P. Gach^{81a}, S. Gadatsch⁵², P. Gadow¹¹³, G. Gagliardi^{53a,53b}, L. G. Gagnon¹⁰⁷, C. Galea^{27b}, B. Galhardo^{137a,137c}, E. J. Gallas¹³², B. J. Gallop¹⁴¹, P. Gallus¹³⁹, G. Galster³⁹, R. Gamboa Goni⁹⁰, K. K. Gan¹²³, S. Ganguly¹⁷⁷, Y. Gao⁸⁸, Y. S. Gao^{150,n}, C. García¹⁷¹, J. E. García Navarro¹⁷¹, J. A. García Pascual^{15a}, M. Garcia-Sciveres¹⁸, R. W. Gardner³⁶, N. Garelli¹⁵⁰, V. Garonne¹³¹, K. Gasnikova⁴⁴, A. Gaudiello^{53a,53b}, G. Gaudio^{68a}, I. L. Gavrilenko¹⁰⁸, A. Gavriluk¹⁰⁹, C. Gay¹⁷², G. Gaycken²⁴, E. N. Gazis¹⁰, C. N. P. Gee¹⁴¹, J. Geisen⁵¹, M. Geisen⁹⁷, M. P. Geisler^{59a}, K. Gellerstedt^{43a,43b}, C. Gemme^{53b}, M. H. Genest⁵⁶, C. Geng¹⁰³, S. Gentile^{70a,70b}, C. Gentsos¹⁵⁹, S. George⁹¹, D. Gerbaudo¹⁴, G. Gessner⁴⁵, S. Ghasemi¹⁴⁸, M. Ghasemi Bostanabad¹⁷³, M. Ghneimat²⁴, B. Giacobbe^{23b}, S. Giagu^{70a,70b}, N. Giangiacomi^{23a,23b}, P. Giannetti^{69a}, S. M. Gibson⁹¹, M. Gignac¹⁴³, D. Gillberg³³, G. Gilles¹⁷⁹, D. M. Gingrich^{3,aw}, M. P. Giordani^{64a,64c}, F. M. Giorgi^{23b}, P. F. Giraud¹⁴², P. Giromini⁵⁷, G. Giugliarelli^{64a,64c}, D. Giugni^{66a}, F. Giulì¹³², M. Giuliani^{59b}, S. Gkaitatzis¹⁵⁹, I. Gkialas^{9,k}, E. L. Gkougkousis¹⁴, P. Gkoutoumis¹⁰, L. K. Gladilin¹¹¹, C. Glasman⁹⁶, J. Glatzer¹⁴, P. C. F. Glaysher⁴⁴, A. Glazov⁴⁴, M. Goblirsch-Kolb²⁶, J. Godlewski⁸², S. Goldfarb¹⁰², T. Golling⁵², D. Golubkov¹²¹, A. Gomes^{137a,137b,137d}, R. Goncalves Gama^{78a}, R. Gonçalves^{137a}, G. Gonella⁵⁰, L. Gonella²¹, A. Gongadze⁷⁷, F. Gonnella²¹, J. L. Gonski⁵⁷, S. González de la Hoz¹⁷¹, S. Gonzalez-Sevilla⁵², L. Goossens³⁵, P. A. Gorbounov¹⁰⁹, H. A. Gordon²⁹, B. Gorini³⁵, E. Gorini^{65a,65b}, A. Gorišek⁸⁹, A. T. Goshaw⁴⁷, C. Gössling⁴⁵, M. I. Gostkin⁷⁷, C. A. Gottardo²⁴, C. R. Goudet¹²⁹, D. Goujdami^{34c}, A. G. Goussiou¹⁴⁵, N. Govender^{32b,d}, C. Goy⁵, E. Gozani¹⁵⁷, I. Grabowska-Bold^{81a}, P. O. J. Gradin¹⁶⁹, E. C. Graham⁸⁸, J. Gramling¹⁴⁵, E. Gramstad¹³¹, S. Grancagnolo¹⁹, V. Gratchev¹³⁵, P. M. Gravila^{27f}, C. Gray⁵⁵, H. M. Gray¹⁸, Z. D. Greenwood^{93,al}, C. Grefe²⁴, K. Gregersen⁹², I. M. Gregor⁴⁴, P. Grenier¹⁵⁰, K. Grevtsov⁴⁴, J. Griffiths⁸, A. A. Grillo¹⁴³, K. Grimm^{150,c}, S. Grinstein^{14,ab}, Ph. Gris³⁷, J.-F. Grivaz¹²⁹, S. Groh⁹⁷, E. Gross¹⁷⁷, J. Grosse-Knetter⁵¹, G. C. Grossi⁹³, Z. J. Grout⁹², C. Grud¹⁰³, A. Grummer¹¹⁶, L. Guan¹⁰³, W. Guan¹⁷⁸, J. Guenther³⁵, A. Guerguichon¹²⁹, F. Guescini^{165a}, D. Guest¹⁶⁸, R. Gugel⁵⁰, B. Gui¹²³, T. Guillemin⁵, S. Guindon³⁵, U. Gul⁵⁵, C. Gumpert³⁵, J. Guo^{58c}, W. Guo¹⁰³, Y. Guo^{58a,u}, Z. Guo⁹⁹, R. Gupta⁴¹, S. Gurbuz^{12c}, G. Gustavino¹²⁵, B. J. Gutelman¹⁵⁷, P. Gutierrez¹²⁵, C. Gutsche⁹², C. Guyot¹⁴², M. P. Guzik^{81a}, C. Gwenlan¹³², C. B. Gwilliam⁸⁸, A. Haas¹²², C. Haber¹⁸, H. K. Hadavand⁸, N. Haddad^{34e}, A. Hadeef^{58a}, S. Hageböck²⁴,

M. Hagihara¹⁶⁶, H. Hakobyan^{181,*}, M. Haleem¹⁷⁴, J. Haley¹²⁶, G. Halladjian¹⁰⁴, G. D. Hallelwell⁹⁹, K. Hamacher¹⁷⁹, P. Hamal¹²⁷, K. Hamano¹⁷³, A. Hamilton^{32a}, G. N. Hamity¹⁴⁶, K. Han^{58a.ak}, L. Han^{58a}, S. Han^{15d}, K. Hanagaki^{79,x}, M. Hance¹⁴³, D. M. Handl¹¹², B. Haney¹³⁴, R. Hankache¹³³, P. Hanke^{59a}, E. Hansen⁹⁴, J. B. Hansen³⁹, J. D. Hansen³⁹, M. C. Hansen²⁴, P. H. Hansen³⁹, K. Hara¹⁶⁶, A. S. Hard¹⁷⁸, T. Harenberg¹⁷⁹, S. Harkusha¹⁰⁵, P. F. Harrison¹⁷⁵, N. M. Hartmann¹¹², Y. Hasegawa¹⁴⁷, A. Hasib⁴⁸, S. Hassani¹⁴², S. Haug²⁰, R. Hauser¹⁰⁴, L. Hauswald⁴⁶, L. B. Havener³⁸, M. Havranek¹³⁹, C. M. Hawkes²¹, R. J. Hawkings³⁵, D. Hayden¹⁰⁴, C. Hayes¹⁵², C. P. Hays¹³², J. M. Hays⁹⁰, H. S. Hayward⁸⁸, S. J. Haywood¹⁴¹, M. P. Heath⁴⁸, V. Hedberg⁹⁴, L. Heelan⁸, S. Heer²⁴, K. K. Heidegger⁵⁰, J. Heilman³³, S. Heim⁴⁴, T. Heim¹⁸, B. Heinemann^{44.ar}, J. J. Heinrich¹¹², L. Heinrich¹²², C. Heinz⁵⁴, J. Hejbal¹³⁸, L. Helary³⁵, A. Held¹⁷², S. Hellesund¹³¹, S. Hellman^{43a,43b}, C. Helsens³⁵, R. C. W. Henderson⁸⁷, Y. Heng¹⁷⁸, S. Henkelmann¹⁷², A. M. Henriques Correia³⁵, G. H. Herbert¹⁹, H. Herde²⁶, V. Herget¹⁷⁴, Y. Hernández Jiménez^{32c}, H. Herr⁹⁷, G. Herten⁵⁰, R. Hertenberger¹¹², L. Hervas³⁵, T. C. Herwig¹³⁴, G. G. Hesketh⁹², N. P. Hessey^{165a}, J. W. Hetherly⁴¹, S. Higashino⁷⁹, E. Higón-Rodríguez¹⁷¹, K. Hildebrand³⁶, E. Hill¹⁷³, J. C. Hill³¹, K. K. Hill²⁹, K. H. Hiller⁴⁴, S. J. Hillier²¹, M. Hils⁴⁶, I. Hinchliffe¹⁸, M. Hirose¹³⁰, D. Hirschbuehl¹⁷⁹, B. Hiti⁸⁹, O. Hladik¹³⁸, D. R. Hlaluku^{32c}, X. Hoad⁴⁸, J. Hobbs¹⁵², N. Hod^{165a}, M. C. Hodgkinson¹⁴⁶, A. Hoecker³⁵, M. R. Hoferkamp¹¹⁶, F. Hoenig¹¹², D. Hohn²⁴, D. Hohov¹²⁹, T. R. Holmes³⁶, M. Holzbock¹¹², M. Homann⁴⁵, S. Honda¹⁶⁶, T. Honda⁷⁹, T. M. Hong¹³⁶, A. Hönle¹¹³, B. H. Hooberman¹⁷⁰, W. H. Hopkins¹²⁸, Y. Horii¹¹⁵, P. Horn⁴⁶, A. J. Horton¹⁴⁹, L. A. Horyn³⁶, J.-Y. Hostachy⁵⁶, A. Hostiuc¹⁴⁵, S. Hou¹⁵⁵, A. Hoummada^{34a}, J. Howarth⁹⁸, J. Hoya⁸⁶, M. Hrabovsky¹²⁷, J. Hrdinka³⁵, I. Hristova¹⁹, J. Hrivnac¹²⁹, A. Hrynevich¹⁰⁶, T. Hryn'ova⁵, P. J. Hsu⁶², S.-C. Hsu¹⁴⁵, Q. Hu²⁹, S. Hu^{58c}, Y. Huang^{15a}, Z. Hubacek¹³⁹, F. Hubaut⁹⁹, M. Huebner²⁴, F. Huegging²⁴, T. B. Huffman¹³², E. W. Hughes³⁸, M. Huhtinen³⁵, R. F. H. Hunter³³, P. Huo¹⁵², A. M. Hupe³³, N. Huseynov^{77.ah}, J. Huston¹⁰⁴, J. Huth⁵⁷, R. Hyneman¹⁰³, G. Iacobucci⁵², G. Iakovidis²⁹, I. Ibragimov¹⁴⁸, L. Iconomidou-Fayard¹²⁹, Z. Idrissi^{34e}, P. Iengo³⁵, R. Ignazzi³⁹, O. Igonkina^{118.ad}, R. Iguchi¹⁶⁰, T. Iizawa⁵², Y. Ikegami⁷⁹, M. Ikeno⁷⁹, D. Iliadis¹⁵⁹, N. Ilic¹⁵⁰, F. Iltzsche⁴⁶, G. Introzzi^{68a,68b}, M. Iodice^{72a}, K. Iordanidou³⁸, V. Ippolito^{70a,70b}, M. F. Isacson¹⁶⁹, N. Ishijima¹³⁰, M. Ishino¹⁶⁰, M. Ishitsuka¹⁶², C. Issever¹³², S. Istin^{12c.aq}, F. Ito¹⁶⁶, J. M. Iturbe Ponce^{61a}, R. Iuppa^{73a,73b}, A. Ivina¹⁷⁷, H. Iwasaki⁷⁹, J. M. Izen⁴², V. Izzo^{67a}, S. Jabbar³, P. Jacka¹³⁸, P. Jackson¹, R. M. Jacobs²⁴, V. Jain², G. Jäkel¹⁷⁹, K. B. Jakobi⁹⁷, K. Jakobs⁵⁰, S. Jakobsen⁷⁴, T. Jakoubek¹³⁸, D. O. Jamin¹²⁶, D. K. Jana⁹³, R. Jansky⁵², J. Janssen²⁴, M. Janus⁵¹, P. A. Janus^{81a}, G. Jarlskog⁹⁴, N. Javadov^{77.ah}, T. Javůrek⁵⁰, M. Javurkova⁵⁰, F. Jeanneau¹⁴², L. Jeanty¹⁸, J. Jejelava^{156a.ai}, A. Jelinskas¹⁷⁵, P. Jenni^{50.e}, J. Jeong⁴⁴, C. Jeske¹⁷⁵, S. Jézéquel⁵, H. Ji¹⁷⁸, J. Jia¹⁵², H. Jiang⁷⁶, Y. Jiang^{58a}, Z. Jiang^{150.s}, S. Jiggins⁵⁰, F. A. Jimenez Morales³⁷, J. Jimenez Pena¹⁷¹, S. Jin^{15c}, A. Jinaru^{27b}, O. Jinnouchi¹⁶², H. Jivan^{32c}, P. Johansson¹⁴⁶, K. A. Johns⁷, C. A. Johnson⁶³, W. J. Johnson¹⁴⁵, K. Jon-And^{43a,43b}, R. W. L. Jones⁸⁷, S. D. Jones¹⁵³, S. Jones⁷, T. J. Jones⁸⁸, J. Jongmanns^{59a}, P. M. Jorge^{137a,137b}, J. Jovicevic^{165a}, X. Ju¹⁷⁸, J. J. Junggeburth¹¹³, A. Juste Rozas^{14.ab}, A. Kaczmarska⁸², M. Kado¹²⁹, H. Kagan¹²³, M. Kagan¹⁵⁰, T. Kaji¹⁷⁶, E. Kajomovitz¹⁵⁷, C. W. Kalderon⁹⁴, A. Kaluza⁹⁷, S. Kama⁴¹, A. Kamenshchikov¹²¹, L. Kanjir⁸⁹, Y. Kano¹⁶⁰, V. A. Kantserov¹¹⁰, J. Kanzaki⁷⁹, B. Kaplan¹²², L. S. Kaplan¹⁷⁸, D. Kar^{32c}, M. J. Kareem^{165b}, E. Karentzos¹⁰, S. N. Karpov⁷⁷, Z. M. Karpova⁷⁷, V. Kartvelishvili⁸⁷, A. N. Karyukhin¹²¹, K. Kasahara¹⁶⁶, L. Kashif¹⁷⁸, R. D. Kass¹²³, A. Kastanas¹⁵¹, Y. Kataoka¹⁶⁰, C. Kato¹⁶⁰, J. Katzy⁴⁴, K. Kawade⁸⁰, K. Kawagoe⁸⁵, T. Kawamoto¹⁶⁰, G. Kawamura⁵¹, E. F. Kay⁸⁸, V. F. Kazanin^{120a,120b}, R. Keeler¹⁷³, R. Kehoe⁴¹, J. S. Keller³³, E. Kellermann⁹⁴, J. J. Kempster²¹, J. Kendrick²¹, O. Kepka¹³⁸, S. Kersten¹⁷⁹, B. P. Kerševan⁸⁹, R. A. Keyes¹⁰¹, M. Khader¹⁷⁰, F. Khalil-Zada¹³, A. Khanov¹²⁶, A. G. Kharlamov^{120a,120b}, T. Kharlamova^{120a,120b}, A. Khodinov¹⁶³, T. J. Khoo⁵², E. Khramov⁷⁷, J. Khubua^{156b}, S. Kido⁸⁰, M. Kiehn⁵², C. R. Kilby⁹¹, S. H. Kim¹⁶⁶, Y. K. Kim³⁶, N. Kimura^{64a,64c}, O. M. Kind¹⁹, B. T. King⁸⁸, D. Kirchmeier⁴⁶, J. Kirk¹⁴¹, A. E. Kiryunin¹¹³, T. Kishimoto¹⁶⁰, D. Kisielewska^{81a}, V. Kitali⁴⁴, O. Kivernyk⁵, E. Kladiva^{28b.*}, T. Klapdor-Kleingrothaus⁵⁰, M. H. Klein¹⁰³, M. Klein⁸⁸, U. Klein⁸⁸, K. Kleinknecht⁹⁷, P. Klimek¹¹⁹, A. Klimentov²⁹, R. Klingenberg^{45.*}, T. Klingl²⁴, T. Klioutchnikova³⁵, F. F. Klitzner¹¹², P. Kluit¹¹⁸, S. Kluth¹¹³, E. Kneringer⁷⁴, E. B. F. G. Knoops⁹⁹, A. Knue⁵⁰, A. Kobayashi¹⁶⁰, D. Kobayashi⁸⁵, T. Kobayashi¹⁶⁰, M. Kobel⁴⁶, M. Kocian¹⁵⁰, P. Kodys¹⁴⁰, T. Koffas³³, E. Koffeman¹¹⁸, N. M. Köhler¹¹³, T. Koi¹⁵⁰, M. Kolb^{59b}, I. Koletsou⁵, T. Kondo⁷⁹, N. Kondrashova^{58c}, K. Köneke⁵⁰, A. C. König¹¹⁷, T. Kono⁷⁹, R. Konoplich^{122.an}, V. Konstantinides⁹², N. Konstantinidis⁹², B. Konya⁹⁴, R. Kopeliansky⁶³, S. Koperny^{81a}, K. Korcyl⁸², K. Kordas¹⁵⁹, A. Korn⁹², I. Korolkov¹⁴, E. V. Korolkova¹⁴⁶, O. Kortner¹¹³, S. Kortner¹¹³, T. Kosek¹⁴⁰, V. V. Kostyukhin²⁴, A. Kotwal⁴⁷, A. Koulouris¹⁰, A. Kourkoumeli-Charalampidi^{68a,68b}, C. Kourkoumelis⁹, E. Kourlitis¹⁴⁶, V. Kouskoura²⁹, A. B. Kowalewska⁸², R. Kowalewski¹⁷³, T. Z. Kowalski^{81a}, C. Kozakai¹⁶⁰, W. Kozanecki¹⁴², A. S. Kozhin¹²¹, V. A. Kramarenko¹¹¹, G. Kramberger⁸⁹, D. Krasnopevtsev¹¹⁰, M. W. Krasny¹³³, A. Krasznahorkay³⁵, D. Krauss¹¹³, J. A. Kremer^{81a}, J. Kretzschmar⁸⁸, P. Krieger¹⁶⁴, K. Krizka¹⁸, K. Kroeninger⁴⁵, H. Kroha¹¹³, J. Kroll¹³⁸, J. Kroll¹³⁴, J. Krstic¹⁶, U. Kruchonak⁷⁷, H. Krüger²⁴, N. Krumnack⁷⁶, M. C. Kruse⁴⁷, T. Kubota¹⁰², S. Kuday^{4b}, J. T. Kuechler¹⁷⁹, S. Kuehn³⁵, A. Kugel^{59a}, F. Kuger¹⁷⁴, T. Kuhl⁴⁴, V. Kukhtin⁷⁷, R. Kukla⁹⁹, Y. Kulchitsky¹⁰⁵, S. Kuleshov^{144b}, Y. P. Kulinich¹⁷⁰, M. Kuna⁵⁶, T. Kunigo⁸³, A. Kupco¹³⁸, T. Kupfer⁴⁵, O. Kuprash¹⁵⁸, H. Kurashige⁸⁰

L. L. Kurchaninov^{165a}, Y. A. Kurochkin¹⁰⁵, M. G. Kurth^{15d}, E. S. Kuwertz¹⁷³, M. Kuze¹⁶², J. Kvita¹²⁷, T. Kwan¹⁷³, A. La Rosa¹¹³, J. L. La Rosa Navarro^{78d}, L. La Rotonda^{40a,40b}, F. La Ruffa^{40a,40b}, C. Lacasta¹⁷¹, F. Lacava^{70a,70b}, J. Lacey⁴⁴, D. P. J. Lack⁹⁸, H. Lacker¹⁹, D. Lacour¹³³, E. Ladygin⁷⁷, R. Lafaye⁵, B. Laforge¹³³, T. Lagouri^{32c}, S. Lai⁵¹, S. Lammers⁶³, W. Lampl⁷, E. Lançon²⁹, U. Landgraf⁵⁰, M. P. J. Landon⁹⁰, M. C. Lanfermann⁵², V. S. Lang⁴⁴, J. C. Lange¹⁴, R. J. Langenberg³⁵, A. J. Lankford¹⁶⁸, F. Lanni²⁹, K. Lantzsch²⁴, A. Lanza^{68a}, A. Lapertosa^{53a,53b}, S. Laplace¹³³, J. F. Laporte¹⁴², T. Lari^{66a}, F. Lasagni Manghi^{23a,23b}, M. Lassnig³⁵, T. S. Lau^{61a}, A. Laudrain¹²⁹, A. T. Law¹⁴³, P. Laycock⁸⁸, M. Lazzaroni^{66a,66b}, B. Le¹⁰², O. Le Dortz¹³³, E. Le Guirriec⁹⁹, E. P. Le Quilleuc¹⁴², M. LeBlanc⁷, T. LeCompte⁶, F. Ledroit-Guillon⁵⁶, C. A. Lee²⁹, G. R. Lee^{144a}, L. Lee⁵⁷, S. C. Lee¹⁵⁵, B. Lefebvre¹⁰¹, M. Lefebvre¹⁷³, F. Legger¹¹², C. Leggett¹⁸, G. Lehmann Miotto³⁵, W. A. Leight⁴⁴, A. Leisos^{159,y}, M. A. L. Leite^{78d}, R. Leitner¹⁴⁰, D. Lellouch¹⁷⁷, B. Lemmer⁵¹, K. J. C. Leney⁹², T. Lenz²⁴, B. Lenzi³⁵, R. Leone⁷, S. Leone^{69a}, C. Leonidopoulos⁴⁸, G. Lerner¹⁵³, C. Leroy¹⁰⁷, R. Les¹⁶⁴, A. A. J. Lesage¹⁴², C. G. Lester³¹, M. Levchenko¹³⁵, J. Levêque⁵, D. Levin¹⁰³, L. J. Levinson¹⁷⁷, D. Lewis⁹⁰, B. Li¹⁰³, C-Q. Li^{58a,am}, H. Li^{58b}, L. Li^{58c}, Q. Li^{15d}, Q. Y. Li^{58a}, S. Li^{58c,58d}, X. Li^{58c}, Y. Li¹⁴⁸, Z. Liang^{15a}, B. Liberti^{71a}, A. Liblong¹⁶⁴, K. Lie^{61c}, S. Liem¹¹⁸, A. Limosani¹⁵⁴, C. Y. Lin³¹, K. Lin¹⁰⁴, T. H. Lin⁹⁷, R. A. Linck⁶³, B. E. Lindquist¹⁵², A. L. Lioni⁵², E. Lipeles¹³⁴, A. Lipniacka¹⁷, M. Lisovsky^{59b}, T. M. Liss^{170,at}, A. Lister¹⁷², A. M. Litke¹⁴³, J. D. Little⁸, B. Liu⁷⁶, B. L. Liu⁶, H. B. Liu²⁹, H. Liu¹⁰³, J. B. Liu^{58a}, J. K. K. Liu¹³², K. Liu¹³³, M. Liu^{58a}, P. Liu¹⁸, Y. Liu^{15a}, Y. L. Liu^{58a}, Y. W. Liu^{58a}, M. Livan^{68a,68b}, A. Lleres⁵⁶, J. Llorente Merino^{15a}, S. L. Lloyd⁹⁰, C. Y. Lo^{61b}, F. Lo Sterzo⁴¹, E. M. Lobodzinska⁴⁴, P. Loch⁷, F. K. Loebinger⁹⁸, K. M. Loew²⁶, T. Lohse¹⁹, K. Lohwasser¹⁴⁶, M. Lokajicek¹³⁸, B. A. Long²⁵, J. D. Long¹⁷⁰, R. E. Long⁸⁷, L. Longo^{65a,65b}, K. A.Looper¹²³, J. A. Lopez^{144b}, I. Lopez Paz¹⁴, A. Lopez Solis¹³³, J. Lorenz¹¹², N. Lorenzo Martinez⁵, M. Losada²², P. J. Lösel¹¹², A. Lösle⁵⁰, X. Lou⁴⁴, X. Lou^{15a}, A. Lounis¹²⁹, J. Love⁶, P. A. Love⁸⁷, J. J. Lozano Bahilo¹⁷¹, H. Lu^{61a}, N. Lu¹⁰³, Y. J. Lu⁶², H. J. Lubatti¹⁴⁵, C. Luci^{70a,70b}, A. Lucotte⁵⁶, C. Luedtke⁵⁰, F. Luehring⁶³, I. Luise¹³³, W. Lukas⁷⁴, L. Luminari^{70a}, B. Lund-Jensen¹⁵¹, M. S. Lutz¹⁰⁰, P. M. Luzi¹³³, D. Lynn²⁹, R. Lysak¹³⁸, E. Lytken⁹⁴, F. Lyu^{15a}, V. Lyubushkin⁷⁷, H. Ma²⁹, L. L. Ma^{58b}, Y. Ma^{58b}, G. Maccarrone⁴⁹, A. Macchiolo¹¹³, C. M. Macdonald¹⁴⁶, J. Machado Miguens^{134,137b}, D. Madaffari¹⁷¹, R. Madar³⁷, W. F. Mader⁴⁶, A. Madsen⁴⁴, N. Madysa⁴⁶, J. Maeda⁸⁰, S. Maeland¹⁷, T. Maeno²⁹, A. S. Maevskiy¹¹¹, V. Magerl⁵⁰, C. Maidantchik^{78b}, T. Maier¹¹², A. Maio^{137a,137b,137d}, O. Majersky^{28a}, S. Majewski¹²⁸, Y. Makida⁷⁹, N. Makovec¹²⁹, B. Malaescu¹³³, Pa. Malecki⁸², V. P. Maleev¹³⁵, F. Malek⁵⁶, U. Mallik⁷⁵, D. Malon⁶, C. Malone³¹, S. Maltezos¹⁰, S. Malyukov³⁵, J. Mamuzic¹⁷¹, G. Mancini⁴⁹, I. Mandić⁸⁹, J. Maneira^{137a}, L. Manhaes de Andrade Filho^{78a}, J. Manjarres Ramos⁴⁶, K. H. Mankinen⁹⁴, A. Mann¹¹², A. Manousos⁷⁴, B. Mansoulie¹⁴², J. D. Mansour^{15a}, M. Mantoani⁵¹, S. Manzoni^{66a,66b}, G. Marceca³⁰, L. March⁵², L. Marchese¹³², G. Marchiori¹³³, M. Marcisovsky¹³⁸, C. A. Marin Tobon³⁵, M. Marjanovic³⁷, D. E. Marley¹⁰³, F. Marroquim^{78b}, Z. Marshall¹⁸, M. U. F. Martensson¹⁶⁹, S. Marti-Garcia¹⁷¹, C. B. Martin¹²³, T. A. Martin¹⁷⁵, V. J. Martin⁴⁸, B. Martin dit Latour¹⁷, M. Martinez^{14,ab}, V. I. Martinez Outschoorn¹⁰⁰, S. Martin-Haugh¹⁴¹ and V. S. Martoiu^{27b}, A. C. Martyniuk⁹², A. Marzin³⁵, L. Masetti⁹⁷, T. Mashimo¹⁶⁰, R. Mashinistov¹⁰⁸, J. Masik⁹⁸, A. L. Maslennikov^{120a,120b}, L. H. Mason¹⁰², L. Massa^{71a,71b}, P. Mastrandrea⁵, A. Mastroberardino^{40a,40b}, T. Masubuchi¹⁶⁰, P. Mättig¹⁷⁹, J. Maurer^{27b}, B. Maček⁸⁹, S. J. Maxfield⁸⁸, D. A. Maximov^{120a,120b}, R. Mazini¹⁵⁵, I. Maznas¹⁵⁹, S. M. Mazza¹⁴³, N. C. Mc Fadden¹¹⁶, G. Mc Goldrick¹⁶⁴, S. P. Mc Kee¹⁰³, A. McCarn¹⁰³, T. G. McCarthy¹¹³, L. I. McClymont⁹², E. F. McDonald¹⁰², J. A. McFayden³⁵, G. Mchedlidze⁵¹, M. A. McKay⁴¹, K. D. McLean¹⁷³, S. J. McMahon¹⁴¹, P. C. McNamara¹⁰², C. J. McNicol¹⁷⁵, R. A. McPherson^{173,af}, J. E. Mdhluli^{32c}, Z. A. Meadows¹⁰⁰, S. Meehan¹⁴⁵, T. M. Megy⁵⁰, S. Mehlhase¹¹², A. Mehta⁸⁸, T. Meideck⁵⁶, B. Meirose⁴², D. Melini^{171,i}, B. R. Mellado Garcia^{32c}, J. D. Mellenthin⁵¹, M. Melo^{28a}, F. Meloni²⁰, A. Melzer²⁴, S. B. Menary⁹⁸, E. D. Mendes Gouveia^{137a}, L. Meng⁸⁸, X. T. Meng¹⁰³, A. Mengarelli^{23a,23b}, S. Menke¹¹³, E. Meoni^{40a,40b}, S. Mergelmeyer¹⁹, C. Merlassino²⁰, P. Mermod⁵², L. Merola^{67a,67b}, C. Meroni^{66a}, F. S. Merritt³⁶, A. Messina^{70a,70b}, J. Metcalfe⁶, A. S. Mete¹⁶⁸, C. Meyer¹³⁴, J. Meyer¹⁵⁷, J-P. Meyer¹⁴², H. Meyer Zu Theenhausen^{59a}, F. Miano¹⁵³, R. P. Middleton¹⁴¹, L. Mijović⁴⁸, G. Mikenberg¹⁷⁷, M. Míkštíkova¹³⁸, M. Mikuž⁸⁹, M. Milesi¹⁰², A. Milic¹⁶⁴, D. A. Millar⁹⁰, D. W. Miller³⁶, A. Milov¹⁷⁷, D. A. Milstead^{43a,43b}, A. A. Minaenko¹²¹, I. A. Minashvili^{156b}, A. I. Mincer¹²², B. Mindur^{81a}, M. Mineev⁷⁷, Y. Minegishi¹⁶⁰, Y. Ming¹⁷⁸, L. M. Mir¹⁴, A. Mirto^{65a,65b}, K. P. Mistry¹³⁴, T. Mitani¹⁷⁶, J. Mitrevski¹¹², V. A. Mitsou¹⁷¹, A. Miucci²⁰, P. S. Miyagawa¹⁴⁶, A. Mizukami⁷⁹, J. U. Mjörnmark⁹⁴, T. Mkrtychyan¹⁸¹, M. Mlynarikova¹⁴⁰, T. Moa^{43a,43b}, K. Mochizuki¹⁰⁷, P. Mogg⁵⁰, S. Mohapatra³⁸, S. Molander^{43a,43b}, R. Moles-Valls²⁴, M. C. Mondragon¹⁰⁴, K. Mönig⁴⁴, J. Monk³⁹, E. Monnier⁹⁹, A. Montalbano¹⁴⁹, J. Montejo Berlingen³⁵, F. Monticelli⁸⁶, S. Monzani^{66a}, R. W. Moore³, N. Morange¹²⁹, D. Moreno²², M. Moreno Llácer³⁵, P. Morettini^{53b}, M. Morgenstern¹¹⁸, S. Morgenstern³⁵, D. Mori¹⁴⁹, T. Mori¹⁶⁰, M. Morii⁵⁷, M. Morinaga¹⁷⁶, V. Morisbak¹³¹, A. K. Morley³⁵, G. Mornacchi³⁵, A. P. Morris⁹², J. D. Morris⁹⁰, L. Morvaj¹⁵², P. Moschovakos¹⁰, M. Mosidze^{156b}, H. J. Moss¹⁴⁶, J. Moss^{150,o}, K. Motohashi¹⁶², R. Mount¹⁵⁰, E. Mountricha³⁵, E. J. W. Moyse¹⁰⁰, S. Muanza⁹⁹, F. Mueller¹¹³, J. Mueller¹³⁶, R. S. P. Mueller¹¹², D. Muenstermann⁸⁷, P. Mullen⁵⁵,

G. A. Mullier²⁰, F. J. Munoz Sanchez⁹⁸, P. Murin^{28b}, W. J. Murray^{175,141}, A. Murrone^{66a,66b}, M. Muškinja⁸⁹, C. Mwewa^{32a}, A. G. Myagkov^{121,ao}, J. Myers¹²⁸, M. Myska¹³⁹, B. P. Nachman¹⁸, O. Nackenhorst⁴⁵, K. Nagai¹³², K. Nagano⁷⁹, Y. Nagasaka⁶⁰, K. Nagata¹⁶⁶, M. Nagel⁵⁰, E. Nagy⁹⁹, A. M. Nairz³⁵, Y. Nakahama¹¹⁵, K. Nakamura⁷⁹, T. Nakamura¹⁶⁰, I. Nakano¹²⁴, H. Nanjo¹³⁰, F. Napolitano^{59a}, R. F. Naranjo Garcia⁴⁴, R. Narayan¹¹, D. I. Narrias Villar^{59a}, I. Naryshkin¹³⁵, T. Naumann⁴⁴, G. Navarro²², R. Nayyar⁷, H. A. Neal^{103,*}, P. Y. Nechaeva¹⁰⁸, T. J. Neep¹⁴², A. Negri^{68a,68b}, M. Negrini^{23b}, S. Nektarijevic¹¹⁷, C. Nellist⁵¹, M. E. Nelson¹³², S. Nemecek¹³⁸, P. Nemethy¹²², M. Nessi^{35,g}, M. S. Neubauer¹⁷⁰, M. Neumann¹⁷⁹, P. R. Newman²¹, T. Y. Ng^{61c}, Y. S. Ng¹⁹, H. D. N. Nguyen⁹⁹, T. Nguyen Manh¹⁰⁷, E. Nibigira³⁷, R. B. Nickerson¹³², R. Nicolaidou¹⁴², J. Nielsen¹⁴³, N. Nikiforou¹¹, V. Nikolaenko^{121,ao}, I. Nikolic-Audit¹³³, K. Nikolopoulos²¹, P. Nilsson²⁹, Y. Ninomiya⁷⁹, A. Nisati^{70a}, N. Nishu^{58c}, R. Nisius¹¹³, I. Nitsche⁴⁵, T. Nitta¹⁷⁶, T. Nobe¹⁶⁰, Y. Noguchi⁸³, M. Nomachi¹³⁰, I. Nomidis¹³³, M. A. Nomura²⁹, T. Nooney⁹⁰, M. Nordberg³⁵, N. Norjoharuddeen¹³², T. Novak⁸⁹, O. Novgorodova⁴⁶, R. Novotny¹³⁹, M. Nozaki⁷⁹, L. Nozka¹²⁷, K. Ntekas¹⁶⁸, E. Nurse⁹², F. Nuti¹⁰², F. G. Oakham^{33,aw}, H. Oberlack¹¹³, T. Obermann²⁴, J. Ocariz¹³³, A. Ochi⁸⁰, I. Ochoa³⁸, J. P. Ochoa-Ricoux^{144a}, K. O'Connor²⁶, S. Oda⁸⁵, S. Odaka⁷⁹, A. Oh⁹⁸, S. H. Oh⁴⁷, C. C. Ohm¹⁵¹, H. Oide^{53a,53b}, H. Okawa¹⁶⁶, Y. Okazaki⁸³, Y. Okumura¹⁶⁰, T. Okuyama⁷⁹, A. Olariu^{27b}, L. F. Oleiro Seabra^{137a}, S. A. Olivares Pino^{144a}, D. Oliveira Damazio²⁹, J. L. Oliver¹, M. J. R. Olsson³⁶, A. Olszewski⁸², J. Olszowska⁸², D. C. O'Neil¹⁴⁹, A. Onofre^{137a,137e}, K. Onogi¹¹⁵, P. U. E. Onyisi¹¹, H. Oppen¹³¹, M. J. Oreglia³⁶, Y. Oren¹⁵⁸, D. Orestano^{72a,72b}, E. C. Orgill⁹⁸, N. Orlando^{61b}, A. A. O'Rourke⁴⁴, R. S. Ori¹⁶⁴, B. Osculati^{53a,53b,*}, V. O'Shea⁵⁵, R. Ospanov^{58a}, G. Otero y Garzon³⁰, H. Otono⁸⁵, M. Ouchrif^{34d}, F. Ould-Saada¹³¹, A. Ouraou¹⁴², Q. Ouyang^{15a}, M. Owen⁵⁵, R. E. Owen²¹, V. E. Ozcan^{12c}, N. Ozturk⁸, J. Pacalt¹²⁷, H. A. Pacey³¹, K. Pachal¹⁴⁹, A. Pacheco Pages¹⁴, L. Pacheco Rodriguez¹⁴², C. Padilla Aranda¹⁴, S. Pagan Griso¹⁸, M. Paganini¹⁸⁰, G. Palacino⁶³, S. Palazzo^{40a,40b}, S. Palestini³⁵, M. Palka^{81b}, D. Pallin³⁷, I. Panagoulas¹⁰, C. E. Pandini³⁵, J. G. Panduro Vazquez⁹¹, P. Pani³⁵, G. Panizzo^{64a,64c}, L. Paolozzi⁵², T. D. Papadopoulou¹⁰, K. Papageorgiou^{9,k}, A. Paramonov⁶, D. Paredes Hernandez^{61b}, B. Parida^{58c}, A. J. Parker⁸⁷, K. A. Parker⁴⁴, M. A. Parker³¹, F. Parodi^{53a,53b}, J. A. Parsons³⁸, U. Parzefall⁵⁰, V. R. Pascuzzi¹⁶⁴, J. M. P. Pasner¹⁴³, E. Pasqualucci^{70a}, S. Passaggio^{53b}, F. Pastore⁹¹, P. Pasuwan^{43a,43b}, S. Pataria⁹⁷, J. R. Pater⁹⁸, A. Pathak^{178,1}, T. Pauly³⁵, B. Pearson¹¹³, M. Pedersen¹³¹, L. Pedraza Diaz¹¹⁷, S. Pedraza Lopez¹⁷¹, R. Pedro^{137a,137b}, S. V. Peleganchuk^{120a,120b}, O. Penc¹³⁸, C. Peng^{15d}, H. Peng^{58a}, B. S. Peralva^{78a}, M. M. Perego¹⁴², A. P. Pereira Peixoto^{137a}, D. V. Perepelitsa²⁹, F. Peri¹⁹, L. Perini^{66a,66b}, H. Pernegger³⁵, S. Perrella^{67a,67b}, V. D. Peshekhonov^{77,*}, K. Peters⁴⁴, R. F. Y. Peters⁹⁸, B. A. Petersen³⁵, T. C. Petersen³⁹, E. Petit⁵⁶, A. Petridis¹, C. Petridou¹⁵⁹, P. Petroff¹²⁹, E. Petrolo^{70a}, M. Petrov¹³², F. Petrucci^{72a,72b}, M. Pettee¹⁸⁰, N. E. Pettersson¹⁰⁰, A. Peyaud¹⁴², R. Pezoa^{144b}, T. Pham¹⁰², F. H. Phillips¹⁰⁴, P. W. Phillips¹⁴¹, G. Piacquadio¹⁵², E. Pianori¹⁸, A. Picazio¹⁰⁰, M. A. Pickering¹³², R. Piegai³⁰, J. E. Pilcher³⁶, A. D. Pilkington⁹⁸, M. Pinamonti^{71a,71b}, J. L. Pinfold³, M. Pitt¹⁷⁷, M.-A. Pleier²⁹, V. Pleskot¹⁴⁰, E. Plotnikova⁷⁷, D. Pluth⁷⁶, P. Podberczko^{120a,120b}, R. Poettgen⁹⁴, R. Poggi⁵², L. Poggioli¹²⁹, I. Pogrebnyak¹⁰⁴, D. Pohl²⁴, I. Pokharel⁵¹, G. Polesello^{68a}, A. Poley⁴⁴, A. Policicchio^{40a,40b}, R. Polifka³⁵, A. Polini^{23b}, C. S. Pollard⁴⁴, V. Polychronakos²⁹, D. Ponomarenko¹¹⁰, L. Pontecorvo³⁵, G. A. Popeneciu^{27d}, D. M. Portillo Quintero¹³³, S. Pospisil¹³⁹, K. Potamianos⁴⁴, I. N. Potrap⁷⁷, C. J. Potter³¹, H. Potti¹¹, T. Poulsen⁹⁴, J. Poveda³⁵, T. D. Powell¹⁴⁶, M. E. Pozo Astigarraga³⁵, P. Pralavorio⁹⁹, S. Prell⁷⁶, D. Price⁹⁸, M. Primavera^{65a}, S. Prince¹⁰¹, N. Proklova¹¹⁰, K. Prokofiev^{61c}, F. Prokoshin^{144b}, S. Protopopescu²⁹, J. Proudfoot⁶, M. Przybycien^{81a}, A. Puri¹⁷⁰, P. Puzo¹²⁹, J. Qian¹⁰³, Y. Qin⁹⁸, A. Quadt⁵¹, M. Queitsch-Maitland⁴⁴, A. Qureshi¹, P. Rados¹⁰², F. Ragusa^{66a,66b}, G. Rahal⁹⁵, J. A. Raine⁹⁸, S. Rajagopalan²⁹, A. Ramirez Morales⁹⁰, T. Rashid¹²⁹, S. Raspopov⁵, M. G. Ratti^{66a,66b}, D. M. Rauch⁴⁴, F. Rauscher¹¹², S. Rave⁹⁷, B. Ravina¹⁴⁶, I. Ravinovich¹⁷⁷, J. H. Rawling⁹⁸, M. Raymond³⁵, A. L. Read¹³¹, N. P. Readioff⁵⁶, M. Reale^{65a,65b}, D. M. Rebuffi^{68a,68b}, A. Redelbach¹⁷⁴, G. Redlinger²⁹, R. Reece¹⁴³, R. G. Reed^{32c}, K. Reeves⁴², L. Rehnisch¹⁹, J. Reichert¹³⁴, A. Reiss⁹⁷, C. Rembsen³⁵, H. Ren^{15d}, M. Rescigno^{70a}, S. Resconi^{66a}, E. D. Resseguie¹³⁴, S. Rettie¹⁷², E. Reynolds²¹, O. L. Rezanova^{120a,120b}, P. Reznicek¹⁴⁰, R. Richter¹¹³, S. Richter⁹², E. Richter-Was^{81b}, O. Ricken²⁴, M. Ridel¹³³, P. Rieck¹¹³, C. J. Riegel¹⁷⁹, O. Rifki⁴⁴, M. Rijssenbeek¹⁵², A. Rimoldi^{68a,68b}, M. Rimoldi²⁰, L. Rinaldi^{23b}, G. Ripellino¹⁵¹, B. Ristić⁸⁷, E. Ritsch³⁵, I. Riu¹⁴, J. C. Rivera Vergara^{144a}, F. Rizatdinova¹²⁶, E. Rizvi⁹⁰, C. Rizzi¹⁴, R. T. Roberts⁹⁸, S. H. Robertson^{101,af}, A. Robichaud-Veronneau¹⁰¹, D. Robinson³¹, J. E. M. Robinson⁴⁴, A. Robson⁵⁵, E. Rocco⁹⁷, C. Roda^{69a,69b}, Y. Rodina⁹⁹, S. Rodriguez Bosca¹⁷¹, A. Rodriguez Perez¹⁴, D. Rodriguez Rodriguez¹⁷¹, A. M. Rodriguez Vera^{165b}, S. Roe³⁵, C. S. Rogan⁵⁷, O. Röhne¹³¹, R. Röhrig¹¹³, C. P. A. Roland⁶³, J. Roloff⁵⁷, A. Romaniouk¹¹⁰, M. Romano^{23a,23b}, N. Rompotis⁸⁸, M. Ronzani¹²², L. Roos¹³³, S. Rosati^{70a}, K. Rosbach⁵⁰, P. Rose¹⁴³, N.-A. Rosien⁵¹, E. Rossi^{67a,67b}, L. P. Rossi^{53b}, L. Rossini^{66a,66b}, J. H. N. Rosten³¹, R. Rosten¹⁴, M. Rotaru^{27b}, J. Rothberg¹⁴⁵, D. Rousseau¹²⁹, D. Roy^{32c}, A. Rozanov⁹⁹, Y. Rozen¹⁵⁷, X. Ruan^{32c}, F. Rubbo¹⁵⁰, F. Rühr⁵⁰, A. Ruiz-Martinez³³, Z. Rurikova⁵⁰, N. A. Rusakovich⁷⁷, H. L. Russell¹⁰¹, J. P. Rutherford⁷, N. Ruthmann³⁵, E. M. Rüttinger^{44,m}, Y. F. Ryabov¹³⁵, M. Rybar¹⁷⁰, G. Rybkin¹²⁹, S. Ryu⁶, A. Ryzhov¹²¹, G. F. Rzehorz⁵¹, P. Sabatini⁵¹, G. Sabato¹¹⁸, S. Sacerdoti¹²⁹, H. F.-W. Sadrozinski¹⁴³, R. Sadykov⁷⁷,

F. Safai Tehrani^{70a}, P. Saha¹¹⁹, M. Sahinsoy^{59a}, A. Sahu¹⁷⁹, M. Saimpert⁴⁴, M. Saito¹⁶⁰, T. Saito¹⁶⁰, H. Sakamoto¹⁶⁰, A. Sakharov^{122,an}, D. Salamani⁵², G. Salamanna^{72a,72b}, J. E. Salazar Loyola^{144b}, D. Salek¹¹⁸, P. H. Sales De Bruin¹⁶⁹, D. Salihagic¹¹³, A. Salnikov¹⁵⁰, J. Salt¹⁷¹, D. Salvatore^{40a,40b}, F. Salvatore¹⁵³, A. Salvucci^{61a,61b,61c}, A. Salzburger³⁵, D. Sammel⁵⁰, D. Sampsonidis¹⁵⁹, D. Sampsonidou¹⁵⁹, J. Sánchez¹⁷¹, A. Sanchez Pineda^{64a,64c}, H. Sandaker¹³¹, C. O. Sander⁴⁴, M. Sandhoff¹⁷⁹, C. Sandoval²², D. P. C. Sankey¹⁴¹, M. Sannino^{53b,53a}, Y. Sano¹¹⁵, A. Sansoni⁴⁹, C. Santoni³⁷, H. Santos^{137a}, I. Santoyo Castillo¹⁵³, A. Sapronov⁷⁷, J. G. Saraiva^{137a,137d}, O. Sasaki⁷⁹, K. Sato¹⁶⁶, E. Sauvan⁵, P. Savard^{164,aw}, N. Savic¹¹³, R. Sawada¹⁶⁰, C. Sawyer¹⁴¹, L. Sawyer^{93,al}, C. Sbarra^{23b}, A. Sbrizzi^{23a,23b}, T. Scanlon⁹², J. Schaarschmidt¹⁴⁵, P. Schacht¹¹³, B. M. Schachtner¹¹², D. Schaefer³⁶, L. Schaefer¹³⁴, J. Schaeffer⁹⁷, S. Schaepe³⁵, U. Schäfer⁹⁷, A. C. Schaffer¹²⁹, D. Schaile¹¹², R. D. Schamberger¹⁵², N. Scharmberg⁹⁸, V. A. Schegelsky¹³⁵, D. Scheirich¹⁴⁰, F. Schenck¹⁹, M. Schernau¹⁶⁸, C. Schiavi^{53b,53a}, S. Schier¹⁴³, L. K. Schildgen²⁴, Z. M. Schillaci²⁶, E. J. Schioppa³⁵, M. Schioppa^{40a,40b}, K. E. Schleicher⁵⁰, S. Schlenker³⁵, K. R. Schmidt-Sommerfeld¹¹³, K. Schmieden³⁵, C. Schmitt⁹⁷, S. Schmitt⁴⁴, S. Schmitz⁹⁷, U. Schnoor⁵⁰, L. Schoeffel¹⁴², A. Schoening^{59b}, E. Schopf²⁴, M. Schott⁹⁷, J. F. P. Schouwenberg¹¹⁷, J. Schovancova³⁵, S. Schramm⁵², A. Schulte⁹⁷, H-C. Schultz-Coulon^{59a}, M. Schumacher⁵⁰, B. A. Schumm¹⁴³, Ph. Schune¹⁴², A. Schwartzman¹⁵⁰, T. A. Schwarz¹⁰³, H. Schweiger⁹⁸, Ph. Schwemling¹⁴², R. Schwienhorst¹⁰⁴, A. Sciandra²⁴, G. Sciolla²⁶, M. Scornajenghi^{40a,40b}, F. Scuri^{69a}, F. Scutti¹⁰², L. M. Scyboz¹¹³, J. Searcy¹⁰³, C. D. Sebastiani^{70a,70b}, P. Seema²⁴, S. C. Seidel¹¹⁶, A. Seiden¹⁴³, T. Seiss³⁶, J. M. Seixas^{78b}, G. Sekhniaidze^{67a}, K. Sekhon¹⁰³, S. J. Sekula⁴¹, N. Semprini-Cesari^{23a,23b}, S. Sen⁴⁷, S. Senkin³⁷, C. Serfon¹³¹, L. Serin¹²⁹, L. Serkin^{64a,64b}, M. Sessa^{72a,72b}, H. Severini¹²⁵, F. Sforza¹⁶⁷, A. Sfyrta⁵², E. Shabalina⁵¹, J. D. Shahinian¹⁴³, N. W. Shaikh^{43a,43b}, L. Y. Shan^{15a}, R. Shang¹⁷⁰, J. T. Shank²⁵, M. Shapiro¹⁸, A. S. Sharma¹, A. Sharma¹³², P. B. Shatalov¹⁰⁹, K. Shaw¹⁵³, S. M. Shaw⁹⁸, A. Shcherbakova¹³⁵, Y. Shen¹²⁵, N. Sherafati³³, A. D. Sherman²⁵, P. Sherwood⁹², L. Shi^{155,as}, S. Shimizu⁸⁰, C. O. Shimmin¹⁸⁰, M. Shimojima¹¹⁴, I. P. J. Shipsey¹³², S. Shirabe⁸⁵, M. Shiyakova⁷⁷, J. Shlomi¹⁷⁷, A. Shmeleva¹⁰⁸, D. Shoaleh Saadi¹⁰⁷, M. J. Shochet³⁶, S. Shojaii¹⁰², D. R. Shope¹²⁵, S. Shrestha¹²³, E. Shulga¹¹⁰, P. Sicho¹³⁸, A. M. Sickles¹⁷⁰, P. E. Sidebo¹⁵¹, E. Sideras Haddad^{32c}, O. Sidiropoulou¹⁷⁴, A. Sidoti^{23a,23b}, F. Siegert⁴⁶, Dj. Sijacki¹⁶, J. Silva^{137a}, M. Silva Jr.¹⁷⁸, M. V. Silva Oliveira^{78a}, S. B. Silverstein^{43a}, L. Simic⁷⁷, S. Simion¹²⁹, E. Simioni⁹⁷, M. Simon⁹⁷, P. Sinervo¹⁶⁴, N. B. Sinev¹²⁸, M. Sioli^{23a,23b}, G. Siragusa¹⁷⁴, I. Siral¹⁰³, S. Yu. Sivoklov¹¹¹, J. Sjölin^{43a,43b}, M. B. Skinner⁸⁷, P. Skubic¹²⁵, M. Slater²¹, T. Slavicek¹³⁹, M. Slawinska⁸², K. Sliwa¹⁶⁷, R. Slovak¹⁴⁰, V. Smakhtin¹⁷⁷, B. H. Smart⁵, J. Smiesko^{28a}, N. Smirnov¹¹⁰, S. Yu. Smirnov¹¹⁰, Y. Smirnov¹¹⁰, L. N. Smirnova¹¹¹, O. Smirnova⁹⁴, J. W. Smith⁵¹, M. N. K. Smith³⁸, R. W. Smith³⁸, M. Smizanska⁸⁷, K. Smolek¹³⁹, A. A. Snesarev¹⁰⁸, I. M. Snyder¹²⁸, S. Snyder²⁹, R. Sobie^{173,af}, A. M. Soffa¹⁶⁸, A. Soffer¹⁵⁸, A. Sogaard⁴⁸, D. A. Soh¹⁵⁵, G. Sokhranyii⁸⁹, C. A. Solans Sanchez³⁵, M. Solar¹³⁹, E. Yu. Soldatov¹¹⁰, U. Soldevila¹⁷¹, A. A. Solodkov¹²¹, A. Soloshenko⁷⁷, O. V. Solovyanov¹²¹, V. Solovyev¹³⁵, P. Sommer¹⁴⁶, H. Son¹⁶⁷, W. Song¹⁴¹, A. Sopczak¹³⁹, F. Sopkova^{28b}, D. Sosa^{59b}, C. L. Sotiropoulou^{69a,69b}, S. Sottocornola^{68a,68b}, R. Soualah^{64a,64c,j}, A. M. Soukharev^{120a,120b}, D. South⁴⁴, B. C. Sowden⁹¹, S. Spagnolo^{65a,65b}, M. Spalla¹¹³, M. Spangenberg¹⁷⁵, F. Spanò⁹¹, D. Sperlich¹⁹, F. Spettel¹¹³, T. M. Spieker^{59a}, R. Spighi^{23b}, G. Spigo³⁵, L. A. Spiller¹⁰², D. P. Spiteri⁵⁵, M. Spousta¹⁴⁰, A. Stabile^{66a,66b}, R. Stamen^{59a}, S. Stamm¹⁹, E. Stanecka⁸², R. W. Stanek⁶, C. Stanescu^{72a}, B. Stanislaus¹³², M. M. Stanitzki⁴⁴, B. Stapf¹¹⁸, S. Stapnes¹³¹, E. A. Starchenko¹²¹, G. H. Stark³⁶, J. Stark⁵⁶, S. H. Stark³⁹, P. Staroba¹³⁸, P. Starovoitov^{59a}, S. Stärz³⁵, R. Staszewski⁸², M. Stegler⁴⁴, P. Steinberg²⁹, B. Stelzer¹⁴⁹, H. J. Stelzer³⁵, O. Stelzer-Chilton^{165a}, H. Stenzel⁵⁴, T. J. Stevenson⁹⁰, G. A. Stewart⁵⁵, M. C. Stockton¹²⁸, G. Stoica^{27b}, P. Stolte⁵¹, S. Stonjek¹¹³, A. Straessner⁴⁶, J. Strandberg¹⁵¹, S. Strandberg^{43a,43b}, M. Strauss¹²⁵, P. Strizenc^{28b}, R. Ströhmer¹⁷⁴, D. M. Strom¹²⁸, R. Stroynowski⁴¹, A. Strubig⁴⁸, S. A. Stucci²⁹, B. Stugu¹⁷, J. Stupak¹²⁵, N. A. Styles⁴⁴, D. Su¹⁵⁰, J. Su¹³⁶, S. Suchek^{59a}, Y. Sugaya¹³⁰, M. Suk¹³⁹, V. V. Sulim¹⁰⁸, D. M. S. Sultan⁵², S. Sultansoy^{4c}, T. Sumida⁸³, S. Sun¹⁰³, X. Sun³, K. Suruliz¹⁵³, C. J. E. Suster¹⁵⁴, M. R. Sutton¹⁵³, S. Suzuki⁷⁹, M. Svatos¹³⁸, M. Swiatlowski³⁶, S. P. Swift², A. Sydorenko⁹⁷, I. Sykora^{28a}, T. Sykora¹⁴⁰, D. Ta⁹⁷, K. Tackmann^{44,ac}, J. Taenzer¹⁵⁸, A. Taffard¹⁶⁸, R. Tafirout^{165a}, E. Tahirovic⁹⁰, N. Taiblum¹⁵⁸, H. Takai²⁹, R. Takashima⁸⁴, E. H. Takasugi¹¹³, K. Takeda⁸⁰, T. Takeshita¹⁴⁷, Y. Takubo⁷⁹, M. Talby⁹⁹, A. A. Talyshv^{120a,120b}, J. Tanaka¹⁶⁰, M. Tanaka¹⁶², R. Tanaka¹²⁹, R. Tanioka⁸⁰, B. B. Tannenwald¹²³, S. Tapia Araya^{144b}, S. Tapprogge⁹⁷, A. Tarek Abouelfadl Mohamed¹³³, S. Tarem¹⁵⁷, G. Tarna^{27b,f}, G. F. Tartarelli^{66a}, P. Tas¹⁴⁰, M. Tasevsky¹³⁸, T. Tashiro⁸³, E. Tassi^{40a,40b}, A. Tavares Delgado^{137a,137b}, Y. Tayalati^{34e}, A. C. Taylor¹¹⁶, A. J. Taylor⁴⁸, G. N. Taylor¹⁰², P. T. E. Taylor¹⁰², W. Taylor^{165b}, A. S. Tee⁸⁷, P. Teixeira-Dias⁹¹, D. Temple¹⁴⁹, H. Ten Kate³⁵, P. K. Teng¹⁵⁵, J. J. Teoh¹³⁰, F. Tepel¹⁷⁹, S. Terada⁷⁹, K. Terashi¹⁶⁰, J. Terron⁹⁶, S. Terzo¹⁴, M. Testa⁴⁹, R. J. Teuscher^{164,af}, S. J. Thais¹⁸⁰, T. Thevenaux-Pelzer⁴⁴, F. Thiele³⁹, J. P. Thomas²¹, A. S. Thompson⁵⁵, P. D. Thompson²¹, L. A. Thomsen¹⁸⁰, E. Thomson¹³⁴, Y. Tian³⁸, R. E. Ticse Torres⁵¹, V. O. Tikhomirov^{108,ap}, Yu. A. Tikhonov^{120a,120b}, S. Timoshenko¹¹⁰, P. Tipton¹⁸⁰, S. Tisserant⁹⁹, K. Todome¹⁶², S. Todorova-Nova⁵, S. Todt⁴⁶, J. Tojo⁸⁵, S. Tokár^{28a}, K. Tokushuku⁷⁹, E. Tolley¹²³, K. G. Tomiwa^{32c}, M. Tomoto¹¹⁵, L. Tompkins^{150,s}, K. Toms¹¹⁶, B. Tong⁵⁷, P. Tornambe⁵⁰, E. Torrence¹²⁸,

H. Torres⁴⁶, E. Torró Pastor¹⁴⁵, C. Tosciri¹³², J. Toth^{99,ae}, F. Touchard⁹⁹, D. R. Tovey¹⁴⁶, C. J. Treado¹²², T. Trefzger¹⁷⁴, F. Tresoldi¹⁵³, A. Tricoli²⁹, I. M. Trigger^{165a}, S. Trincaz-Duvoid¹³³, M. F. Tripiana¹⁴, W. Trischuk¹⁶⁴, B. Trocme⁵⁶, A. Trofymov¹²⁹, C. Troncon^{66a}, M. Trovatelli¹⁷³, F. Trovato¹⁵³, L. Truong^{32b}, M. Trzebinski⁸², A. Trzupek⁸², F. Tsai⁴⁴, J. C.-L. Tseng¹³², P. V. Tsiarshka¹⁰⁵, N. Tsirintanis⁹, V. Tsiskaridze¹⁵², E. G. Tskhadadze^{156a}, I. I. Tsukerman¹⁰⁹, V. Tsulaia¹⁸, S. Tsuno⁷⁹, D. Tsybychev¹⁵², Y. Tu^{61b}, A. Tudorache^{27b}, V. Tudorache^{27b}, T. T. Tulbure^{27a}, A. N. Tuna⁵⁷, S. Turchikhin⁷⁷, D. Turgeman¹⁷⁷, I. Turk Cakir^{4b,w}, R. Turra^{66a}, P. M. Tuts³⁸, E. Tzovara⁹⁷, G. Ucchielli^{23a,23b}, I. Ueda⁷⁹, M. Ughetto^{43a,43b}, F. Ukegawa¹⁶⁶, G. Unal³⁵, A. Undrus²⁹, G. Unel¹⁶⁸, F. C. Ungaro¹⁰², Y. Unno⁷⁹, K. Uno¹⁶⁰, J. Urban^{28b}, P. Urquijo¹⁰², P. Urrejola⁹⁷, G. Usai⁸, J. Usui⁷⁹, L. Vacavant⁹⁹, V. Vacek¹³⁹, B. Vachon¹⁰¹, K. O. H. Vadla¹³¹, A. Vaidya⁹², C. Valderanis¹¹², E. Valdes Santurio^{43a,43b}, M. Valente⁵², S. Valentinetti^{23a,23b}, A. Valero¹⁷¹, L. Valéry⁴⁴, R. A. Vallance²¹, A. Vallier⁵, J. A. Valls Ferrer¹⁷¹, T. R. Van Daalen¹⁴, W. Van Den Wollenberg¹¹⁸, H. Van der Graaf¹¹⁸, P. Van Gemmeren⁶, J. Van Nieuwkoop¹⁴⁹, I. Van Vulpen¹¹⁸, M. C. van Woerden¹¹⁸, M. Vanadia^{71a,71b}, W. Vandelli³⁵, A. Vaniachine¹⁶³, P. Vankov¹¹⁸, R. Vari^{70a}, E. W. Varnes⁷, C. Varni^{53b,53a}, T. Varol⁴¹, D. Varouchas¹²⁹, A. Vartapetian⁸, K. E. Varvell¹⁵⁴, G. A. Vasquez^{144b}, J. G. Vasquez¹⁸⁰, F. Vazeille³⁷, D. Vazquez Furelos¹⁴, T. Vazquez Schroeder¹⁰¹, J. Veatch⁵¹, V. Vecchio^{72a,72b}, L. M. Veloce¹⁶⁴, F. Veloso^{137a,137c}, S. Veneziano^{70a}, A. Ventura^{65a,65b}, M. Venturi¹⁷³, N. Venturi³⁵, V. Vercesi^{68a}, M. Verducci^{72a,72b}, C. M. Vergel Infante⁷⁶, W. Verkerke¹¹⁸, A. T. Vermeulen¹¹⁸, J. C. Vermeulen¹¹⁸, M. C. Vetterli^{149,aw}, N. Viaux Maira^{144b}, O. Viazlo⁹⁴, I. Vichou^{170,*}, T. Vickey¹⁴⁶, O. E. Vickey Boeriu¹⁴⁶, G. H. A. Viehhauser¹³², S. Viel¹⁸, L. Vigani¹³², M. Villa^{23a,23b}, M. Villaplana Perez^{66a,66b}, E. Vilucchi⁴⁹, M. G. Vincter³³, V. B. Vinogradov⁷⁷, A. Vishwakarma⁴⁴, C. Vittori^{23a,23b}, I. Vivarelli¹⁵³, S. Vlachos¹⁰, M. Vogel¹⁷⁹, P. Vokac¹³⁹, G. Volpi¹⁴, S. E. von Buddenbrock^{32c}, E. Von Toerne²⁴, V. Vorobel¹⁴⁰, K. Vorobev¹¹⁰, M. Vos¹⁷¹, J. H. Vossebeld⁸⁸, N. Vranjes¹⁶, M. Vranjes Milosavljevic¹⁶, V. Vrba¹³⁹, M. Vreeswijk¹¹⁸, T. Šfiligoj⁸⁹, R. Vuillermet³⁵, I. Vukotic³⁶, T. Ženiš^{28a}, L. Živkovic¹⁶, P. Wagner²⁴, W. Wagner¹⁷⁹, J. Wagner-Kuhr¹¹², H. Wahlberg⁸⁶, S. Wahrmund⁴⁶, K. Wakamiya⁸⁰, V. M. Walbrecht¹¹³, J. Walder⁸⁷, R. Walker¹¹², W. Walkowiak¹⁴⁸, V. Wallangen^{43a,43b}, A. M. Wang⁵⁷, C. Wang^{58b,f}, F. Wang¹⁷⁸, H. Wang¹⁸, H. Wang³, J. Wang¹⁵⁴, J. Wang^{59b}, P. Wang⁴¹, Q. Wang¹²⁵, R.-J. Wang¹³³, R. Wang^{58a}, R. Wang⁶, S. M. Wang¹⁵⁵, W. T. Wang^{58a}, W. Wang^{155,q}, W. X. Wang^{58a,ag}, Y. Wang^{58a,am}, Z. Wang^{58c}, C. Wanotayaroj⁴⁴, A. Warburton¹⁰¹, C. P. Ward³¹, D. R. Wardrope⁹², A. Washbrook⁴⁸, P. M. Watkins²¹, A. T. Watson²¹, M. F. Watson²¹, G. Watts¹⁴⁵, S. Watts⁹⁸, B. M. Waugh⁹², A. F. Webb¹¹, S. Webb⁹⁷, C. Weber¹⁸⁰, M. S. Weber²⁰, S. A. Weber³³, S. M. Weber^{59a}, J. S. Webster⁶, A. R. Weidberg¹³², B. Weinert⁶³, J. Weingarten⁵¹, M. Weirich⁹⁷, C. Weiser⁵⁰, P. S. Wells³⁵, T. Wenaus²⁹, T. Wengler³⁵, S. Wenig³⁵, N. Wermes²⁴, M. D. Werner⁷⁶, P. Werner³⁵, M. Wessels^{59a}, T. D. Weston²⁰, K. Whalen¹²⁸, N. L. Whallon¹⁴⁵, A. M. Wharton⁸⁷, A. S. White¹⁰³, A. White⁸, M. J. White¹, R. White^{144b}, D. Whiteson¹⁶⁸, B. W. Whitmore⁸⁷, F. J. Wickens¹⁴¹, W. Wiedenmann¹⁷⁸, M. WIELERS¹⁴¹, C. WIGLESWORTH³⁹, L. A. M. Wiik-Fuchs⁵⁰, A. Wildauer¹¹³, F. Wilk⁹⁸, H. G. Wilkens³⁵, L. J. Wilkins⁹¹, H. H. Williams¹²⁸, S. Williams¹⁵³, C. Willis¹⁰⁴, S. Willocq¹⁰⁰, J. A. Wilson²¹, I. Wingerter-Seez⁵, E. Winkels¹⁵³, F. Winklmeier¹²⁸, O. J. Winston¹⁵³, B. T. Winter²⁴, M. Wittgen¹⁵⁰, M. Wobisch⁹³, A. Wolf⁹⁷, T. M. H. Wolf¹¹⁸, R. Wolff⁹⁹, M. W. Wolter⁸², H. Wolters^{137a,137c}, V. W. S. Wong¹⁷², N. L. Woods¹⁴³, S. D. Worm²¹, B. K. Wosiek⁸², K. W. Woźniak⁸², K. Wraight⁵⁵, M. Wu³⁶, S. L. Wu¹⁷⁸, X. Wu⁵², Y. Wu^{58a}, T. R. Wyatt⁹⁸, B. M. Wynne⁴⁸, S. Xella³⁹, Z. Xi¹⁰³, L. Xia¹⁷⁵, D. Xu^{15a}, H. Xu^{58a,f}, L. Xu²⁹, T. Xu¹⁴², W. Xu¹⁰³, B. Yabsley¹⁵⁴, S. Yacoub^{32a}, K. Yajima¹³⁰, D. P. Yallup⁹², D. Yamaguchi¹⁶², Y. Yamaguchi¹⁶², A. Yamamoto⁷⁹, T. Yamanaka¹⁶⁰, F. Yamane⁸⁰, M. Yamatani¹⁶⁰, T. Yamazaki¹⁶⁰, Y. Yamazaki⁸⁰, Z. Yan²⁵, H. J. Yang^{58c,58d}, H. T. Yang¹⁸, S. Yang⁷⁵, Y. Yang¹⁶⁰, Z. Yang¹⁷, W.-M. Yao¹⁸, Y. C. Yap⁴⁴, Y. Yasu⁷⁹, E. Yatsenko^{58c}, J. Ye⁴¹, S. Ye²⁹, I. Yeletsikhin⁷⁷, E. Yigitbasi²⁵, E. Yildirim⁹⁷, K. Yorita¹⁷⁶, K. Yoshihara¹³⁴, C. J. S. Young³⁵, C. Young¹⁵⁰, J. Yu⁸, J. Yu⁷⁶, X. Yue^{59a}, S. P. Y. Yuen²⁴, I. Yusuff^{31,a}, B. Zabinski⁸², G. Zacharis¹⁰, E. Zaffaroni⁵², R. Zaidan¹⁴, A. M. Zaitsev^{121,ao}, N. Zakharchuk⁴⁴, J. Zalieckas¹⁷, S. Zambito⁵⁷, D. Zanzi³⁵, D. R. Zaripovas⁵⁵, S. V. Zeißner⁴⁵, C. Zeitnitz¹⁷⁹, G. Zemaityte¹³², J. C. Zeng¹⁷⁰, Q. Zeng¹⁵⁰, O. Zenin¹²¹, D. Zerwas¹²⁹, M. Zgubić¹³², D. F. Zhang^{58b}, D. Zhang¹⁰³, F. Zhang¹⁷⁸, G. Zhang^{58a,ag}, H. Zhang^{15c}, J. Zhang⁶, L. Zhang⁵⁰, L. Zhang^{58a}, M. Zhang¹⁷⁰, P. Zhang^{15c}, R. Zhang^{58a,f}, R. Zhang²⁴, X. Zhang^{58b}, Y. Zhang^{15d}, Z. Zhang¹²⁹, P. Zhao⁴⁷, X. Zhao⁴¹, Y. Zhao^{58b,129,ak}, Z. Zhao^{58a}, A. Zhemchugov⁷⁷, B. Zhou¹⁰³, C. Zhou¹⁷⁸, L. Zhou⁴¹, M. S. Zhou^{15d}, M. Zhou¹⁵², N. Zhou^{58c}, Y. Zhou⁷, C. G. Zhu^{58b}, H. L. Zhu^{58a}, H. Zhu^{15a}, J. Zhu¹⁰³, Y. Zhu^{58a}, X. Zhuang^{15a}, K. Zhukov¹⁰⁸, V. Zhulanov^{120a,120b}, A. Zibell¹⁷⁴, D. Zieminska⁶³, N. I. Zimine⁷⁷, S. Zimmermann⁵⁰, Z. Zinonos¹¹³, M. Zinser⁹⁷, M. Ziolkowski¹⁴⁸, G. Zobernig¹⁷⁸, A. Zoccoli^{23a,23b}, K. Zoch⁵¹, T. G. Zorbas¹⁴⁶, R. Zou³⁶, M. Zur Nedden¹⁹, L. Zwalinski³⁵

¹ Department of Physics, University of Adelaide, Adelaide, Australia

² Physics Department, SUNY Albany, Albany, NY, USA

³ Department of Physics, University of Alberta, Edmonton, AB, Canada

- 4 (a)Department of Physics, Ankara University, Ankara, Turkey; (b)Istanbul Aydin University, Istanbul, Turkey; (c)Division of Physics, TOBB University of Economics and Technology, Ankara, Turkey
- 5 LAPP, Université Grenoble Alpes, Université Savoie Mont Blanc, CNRS/IN2P3, Annecy, France
- 6 High Energy Physics Division, Argonne National Laboratory, Argonne, IL, USA
- 7 Department of Physics, University of Arizona, Tucson, AZ, USA
- 8 Department of Physics, University of Texas at Arlington, Arlington, TX, USA
- 9 Physics Department, National and Kapodistrian University of Athens, Athens, Greece
- 10 Physics Department, National Technical University of Athens, Zografou, Greece
- 11 Department of Physics, University of Texas at Austin, Austin, TX, USA
- 12 (a)Bahcesehir University, Faculty of Engineering and Natural Sciences, Istanbul, Turkey; (b)Istanbul Bilgi University, Faculty of Engineering and Natural Sciences, Istanbul, Turkey; (c)Department of Physics, Bogazici University, Istanbul, Turkey; (d)Department of Physics Engineering, Gaziantep University, Gaziantep, Turkey
- 13 Institute of Physics, Azerbaijan Academy of Sciences, Baku, Azerbaijan
- 14 Institut de Física d'Altes Energies (IFAE), Barcelona Institute of Science and Technology, Barcelona, Spain
- 15 (a)Institute of High Energy Physics, Chinese Academy of Sciences, Beijing, China; (b)Physics Department, Tsinghua University, Beijing, China; (c)Department of Physics, Nanjing University, Nanjing, China; (d)University of Chinese Academy of Science (UCAS), Beijing, China
- 16 Institute of Physics, University of Belgrade, Belgrade, Serbia
- 17 Department for Physics and Technology, University of Bergen, Bergen, Norway
- 18 Physics Division, Lawrence Berkeley National Laboratory and University of California, Berkeley, CA, USA
- 19 Institut für Physik, Humboldt Universität zu Berlin, Berlin, Germany
- 20 Albert Einstein Center for Fundamental Physics and Laboratory for High Energy Physics, University of Bern, Bern, Switzerland
- 21 School of Physics and Astronomy, University of Birmingham, Birmingham, UK
- 22 Centro de Investigaciones, Universidad Antonio Nariño, Bogota, Colombia
- 23 (a)Dipartimento di Fisica e Astronomia, Università di Bologna, Bologna, Italy; (b)INFN Sezione di Bologna, Bologna, Italy
- 24 Physikalisches Institut, Universität Bonn, Bonn, Germany
- 25 Department of Physics, Boston University, Boston, MA, USA
- 26 Department of Physics, Brandeis University, Waltham, MA, USA
- 27 (a)Transilvania University of Brasov, Brasov, Romania; (b)Horia Hulubei National Institute of Physics and Nuclear Engineering, Bucharest, Romania; (c)Department of Physics, Alexandru Ioan Cuza University of Iasi, Iasi, Romania; (d)Physics Department, National Institute for Research and Development of Isotopic and Molecular Technologies, Cluj-Napoca, Romania; (e)University Politehnica Bucharest, Bucharest, Romania; (f)West University in Timisoara, Timisoara, Romania
- 28 (a)Faculty of Mathematics, Physics and Informatics, Comenius University, Bratislava, Slovak Republic; (b)Department of Subnuclear Physics, Institute of Experimental Physics of the Slovak Academy of Sciences, Kosice, Slovak Republic
- 29 Physics Department, Brookhaven National Laboratory, Upton, NY, USA
- 30 Departamento de Física, Universidad de Buenos Aires, Buenos Aires, Argentina
- 31 Cavendish Laboratory, University of Cambridge, Cambridge, UK
- 32 (a)Department of Physics, University of Cape Town, Cape Town, South Africa; (b)Department of Mechanical Engineering Science, University of Johannesburg, Johannesburg, South Africa; (c)School of Physics, University of the Witwatersrand, Johannesburg, South Africa
- 33 Department of Physics, Carleton University, Ottawa, ON, Canada
- 34 (a)Faculté des Sciences Ain Chock, Réseau Universitaire de Physique des Hautes Energies, Université Hassan II, Casablanca, Morocco; (b)Centre National de l'Energie des Sciences Techniques Nucleaires (CNESTEN), Rabat, Morocco; (c)Faculté des Sciences Semlalia, Université Cadi Ayyad, LPHEA-Marrakech, Marrakesh, Morocco; (d)Faculté des Sciences, Université Mohamed Premier and LPTPM, Oujda, Morocco; (e)Faculté des sciences, Université Mohammed V, Rabat, Morocco
- 35 CERN, Geneva, Switzerland
- 36 Enrico Fermi Institute, University of Chicago, Chicago, IL, USA
- 37 LPC, Université Clermont Auvergne, CNRS/IN2P3, Clermont-Ferrand, France
- 38 Nevis Laboratory, Columbia University, Irvington, NY, USA

- ³⁹ Niels Bohr Institute, University of Copenhagen, Copenhagen, Denmark
- ⁴⁰ ^(a)Dipartimento di Fisica, Università della Calabria, Rende, Italy; ^(b)INFN Gruppo Collegato di Cosenza, Laboratori Nazionali di Frascati, Frascati, Italy
- ⁴¹ Physics Department, Southern Methodist University, Dallas, TX, USA
- ⁴² Physics Department, University of Texas at Dallas, Richardson, TX, USA
- ⁴³ ^(a)Department of Physics, Stockholm University, Stockholm, Sweden; ^(b)Oskar Klein Centre, Stockholm, Sweden
- ⁴⁴ Deutsches Elektronen-Synchrotron DESY, Hamburg and Zeuthen, Germany
- ⁴⁵ Lehrstuhl für Experimentelle Physik IV, Technische Universität Dortmund, Dortmund, Germany
- ⁴⁶ Institut für Kern- und Teilchenphysik, Technische Universität Dresden, Dresden, Germany
- ⁴⁷ Department of Physics, Duke University, Durham, NC, USA
- ⁴⁸ SUPA, School of Physics and Astronomy, University of Edinburgh, Edinburgh, UK
- ⁴⁹ INFN e Laboratori Nazionali di Frascati, Frascati, Italy
- ⁵⁰ Physikalisches Institut, Albert-Ludwigs-Universität Freiburg, Freiburg, Germany
- ⁵¹ II. Physikalisches Institut, Georg-August-Universität Göttingen, Göttingen, Germany
- ⁵² Département de Physique Nucléaire et Corpusculaire, Université de Genève, Geneva, Switzerland
- ⁵³ ^(a)Dipartimento di Fisica, Università di Genova, Genoa, Switzerland; ^(b)INFN Sezione di Genova, Genoa, Italy
- ⁵⁴ II. Physikalisches Institut, Justus-Liebig-Universität Giessen, Giessen, Germany
- ⁵⁵ SUPA, School of Physics and Astronomy, University of Glasgow, Glasgow, UK
- ⁵⁶ LPSC, Université Grenoble Alpes, CNRS/IN2P3, Grenoble INP, Grenoble, France
- ⁵⁷ Laboratory for Particle Physics and Cosmology, Harvard University, Cambridge, MA, USA
- ⁵⁸ ^(a)Department of Modern Physics and State Key Laboratory of Particle Detection and Electronics, University of Science and Technology of China, Hefei, China; ^(b)Institute of Frontier and Interdisciplinary Science and Key Laboratory of Particle Physics and Particle Irradiation (MOE), Shandong University, Qingdao, China; ^(c)School of Physics and Astronomy, Shanghai Jiao Tong University, KLPPAC-MoE, SKLPPC, Shanghai, China; ^(d)Tsung-Dao Lee Institute, Shanghai, China
- ⁵⁹ ^(a)Kirchhoff-Institut für Physik, Ruprecht-Karls-Universität Heidelberg, Heidelberg, Germany; ^(b)Physikalisches Institut, Ruprecht-Karls-Universität Heidelberg, Heidelberg, Germany
- ⁶⁰ Faculty of Applied Information Science, Hiroshima Institute of Technology, Hiroshima, Japan
- ⁶¹ ^(a)Department of Physics, Chinese University of Hong Kong, Shatin, N.T., Hong Kong; ^(b)Department of Physics, University of Hong Kong, Hong Kong, China; ^(c)Department of Physics and Institute for Advanced Study, Hong Kong University of Science and Technology, Clear Water Bay, Kowloon, Hong Kong, China
- ⁶² Department of Physics, National Tsing Hua University, Hsinchu, Taiwan
- ⁶³ Department of Physics, Indiana University, Bloomington, IN, USA
- ⁶⁴ ^(a)INFN Gruppo Collegato di Udine, Sezione di Trieste, Udine, Italy; ^(b)ICTP, Trieste, Italy; ^(c)Dipartimento di Chimica, Fisica e Ambiente, Università di Udine, Udine, Italy
- ⁶⁵ ^(a)INFN Sezione di Lecce, Lecce, Italy; ^(b)Dipartimento di Matematica e Fisica, Università del Salento, Lecce, Italy
- ⁶⁶ ^(a)INFN Sezione di Milano, Milan, Italy; ^(b)Dipartimento di Fisica, Università di Milano, Milan, Italy
- ⁶⁷ ^(a)INFN Sezione di Napoli, Naples, Italy; ^(b)Dipartimento di Fisica, Università di Napoli, Naples, Italy
- ⁶⁸ ^(a)INFN Sezione di Pavia, Pavia, Italy; ^(b)Dipartimento di Fisica, Università di Pavia, Pavia, Italy
- ⁶⁹ ^(a)INFN Sezione di Pisa, Pisa, Italy; ^(b)Dipartimento di Fisica E. Fermi, Università di Pisa, Pisa, Italy
- ⁷⁰ ^(a)INFN Sezione di Roma, Rome, Italy; ^(b)Dipartimento di Fisica, Sapienza Università di Roma, Rome, Italy
- ⁷¹ ^(a)INFN Sezione di Roma Tor Vergata, Rome, Italy; ^(b)Dipartimento di Fisica, Università di Roma Tor Vergata, Rome, Italy
- ⁷² ^(a)INFN Sezione di Roma Tre, Rome, Italy; ^(b)Dipartimento di Matematica e Fisica, Università Roma Tre, Rome, Italy
- ⁷³ ^(a)INFN-TIFPA, Povo, Italy; ^(b)Università degli Studi di Trento, Trento, Italy
- ⁷⁴ Institut für Astro- und Teilchenphysik, Leopold-Franzens-Universität, Innsbruck, Austria
- ⁷⁵ University of Iowa, Iowa City, IA, USA
- ⁷⁶ Department of Physics and Astronomy, Iowa State University, Ames, IA, USA
- ⁷⁷ Joint Institute for Nuclear Research, Dubna, Russia
- ⁷⁸ ^(a)Departamento de Engenharia Elétrica, Universidade Federal de Juiz de Fora (UFJF), Juiz de Fora, Brazil; ^(b)Universidade Federal do Rio De Janeiro COPPE/EE/IF, Rio de Janeiro, Brazil; ^(c)Universidade Federal de São João del Rei (UFSJ), São João del Rei, Brazil; ^(d)Instituto de Física, Universidade de São Paulo, São Paulo, Brazil
- ⁷⁹ KEK, High Energy Accelerator Research Organization, Tsukuba, Japan

- 80 Graduate School of Science, Kobe University, Kobe, Japan
- 81 ^(a)Faculty of Physics and Applied Computer Science, AGH University of Science and Technology, Kraków, Poland; ^(b)Marian Smoluchowski Institute of Physics, Jagiellonian University, Kraków, Poland
- 82 Institute of Nuclear Physics Polish Academy of Sciences, Kraków, Poland
- 83 Faculty of Science, Kyoto University, Kyoto, Japan
- 84 Kyoto University of Education, Kyoto, Japan
- 85 Research Center for Advanced Particle Physics and Department of Physics, Kyushu University, Fukuoka, Japan
- 86 Instituto de Física La Plata, Universidad Nacional de La Plata and CONICET, La Plata, Argentina
- 87 Physics Department, Lancaster University, Lancaster, UK
- 88 Oliver Lodge Laboratory, University of Liverpool, Liverpool, UK
- 89 Department of Experimental Particle Physics, Jožef Stefan Institute and Department of Physics, University of Ljubljana, Ljubljana, Slovenia
- 90 School of Physics and Astronomy, Queen Mary University of London, London, UK
- 91 Department of Physics, Royal Holloway University of London, Egham, UK
- 92 Department of Physics and Astronomy, University College London, London, UK
- 93 Louisiana Tech University, Ruston, LA, USA
- 94 Fysiska institutionen, Lunds universitet, Lund, Sweden
- 95 Centre de Calcul de l'Institut National de Physique Nucléaire et de Physique des Particules (IN2P3), Villeurbanne, France
- 96 Departamento de Física Teórica C-15 and CIAFF, Universidad Autónoma de Madrid, Madrid, Spain
- 97 Institut für Physik, Universität Mainz, Mainz, Germany
- 98 School of Physics and Astronomy, University of Manchester, Manchester, UK
- 99 CPPM, Aix-Marseille Université, CNRS/IN2P3, Marseille, France
- 100 Department of Physics, University of Massachusetts, Amherst, MA, USA
- 101 Department of Physics, McGill University, Montreal, QC, Canada
- 102 School of Physics, University of Melbourne, Melbourne, VIC, Australia
- 103 Department of Physics, University of Michigan, Ann Arbor, MI, USA
- 104 Department of Physics and Astronomy, Michigan State University, East Lansing, MI, USA
- 105 B.I. Stepanov Institute of Physics, National Academy of Sciences of Belarus, Minsk, Belarus
- 106 Research Institute for Nuclear Problems of Byelorussian State University, Minsk, Belarus
- 107 Group of Particle Physics, University of Montreal, Montreal, QC, Canada
- 108 P.N. Lebedev Physical Institute of the Russian Academy of Sciences, Moscow, Russia
- 109 Institute for Theoretical and Experimental Physics (ITEP), Moscow, Russia
- 110 National Research Nuclear University MEPhI, Moscow, Russia
- 111 D.V. Skobeltsyn Institute of Nuclear Physics, M.V. Lomonosov Moscow State University, Moscow, Russia
- 112 Fakultät für Physik, Ludwig-Maximilians-Universität München, Munich, Germany
- 113 Max-Planck-Institut für Physik (Werner-Heisenberg-Institut), Munich, Germany
- 114 Nagasaki Institute of Applied Science, Nagasaki, Japan
- 115 Graduate School of Science and Kobayashi-Maskawa Institute, Nagoya University, Nagoya, Japan
- 116 Department of Physics and Astronomy, University of New Mexico, Albuquerque, NM, USA
- 117 Institute for Mathematics, Astrophysics and Particle Physics, Radboud University Nijmegen/Nikhef, Nijmegen, The Netherlands
- 118 Nikhef National Institute for Subatomic Physics and University of Amsterdam, Amsterdam, The Netherlands
- 119 Department of Physics, Northern Illinois University, DeKalb, IL, USA
- 120 ^(a)Budker Institute of Nuclear Physics, SB RAS, Novosibirsk, Russia; ^(b)Novosibirsk State University, Novosibirsk, Russia
- 121 Institute for High Energy Physics of the National Research Centre Kurchatov Institute, Protvino, Russia
- 122 Department of Physics, New York University, New York, NY, USA
- 123 Ohio State University, Columbus, OH, USA
- 124 Faculty of Science, Okayama University, Okayama, Japan
- 125 Homer L. Dodge Department of Physics and Astronomy, University of Oklahoma, Norman, OK, USA
- 126 Department of Physics, Oklahoma State University, Stillwater, OK, USA
- 127 Palacký University, RCPTM, Joint Laboratory of Optics, Olomouc, Czech Republic

- 128 Center for High Energy Physics, University of Oregon, Eugene, OR, USA
- 129 LAL, Université Paris-Sud, CNRS/IN2P3, Université Paris-Saclay, Orsay, France
- 130 Graduate School of Science, Osaka University, Osaka, Japan
- 131 Department of Physics, University of Oslo, Oslo, Norway
- 132 Department of Physics, Oxford University, Oxford, UK
- 133 LPNHE, Sorbonne Université, Paris Diderot Sorbonne Paris Cité, CNRS/IN2P3, Paris, France
- 134 Department of Physics, University of Pennsylvania, Philadelphia, PA, USA
- 135 Konstantinov Nuclear Physics Institute of National Research Centre “Kurchatov Institute”, PNPI, St. Petersburg, Russia
- 136 Department of Physics and Astronomy, University of Pittsburgh, Pittsburgh, PA, USA
- 137 ^(a)Laboratório de Instrumentação e Física Experimental de Partículas-LIP, Lisbon, Portugal; ^(b)Departamento de Física, Faculdade de Ciências, Universidade de Lisboa, Lisbon, Portugal; ^(c)Departamento de Física, Universidade de Coimbra, Coimbra, Portugal; ^(d)Centro de Física Nuclear da Universidade de Lisboa, Lisbon, Portugal; ^(e)Departamento de Física, Universidade do Minho, Braga, Portugal; ^(f)Departamento de Física Teórica y del Cosmos, Universidad de Granada, Granada, Spain; ^(g)Dep Física and CEFITEC of Faculdade de Ciências e Tecnologia, Universidade Nova de Lisboa, Caparica, Portugal
- 138 Institute of Physics, Academy of Sciences of the Czech Republic, Prague, Czech Republic
- 139 Czech Technical University in Prague, Prague, Czech Republic
- 140 Faculty of Mathematics and Physics, Charles University, Prague, Czech Republic
- 141 Particle Physics Department, Rutherford Appleton Laboratory, Didcot, UK
- 142 IRFU, CEA, Université Paris-Saclay, Gif-sur-Yvette, France
- 143 Santa Cruz Institute for Particle Physics, University of California Santa Cruz, Santa Cruz, CA, USA
- 144 ^(a)Departamento de Física, Pontificia Universidad Católica de Chile, Santiago, Chile; ^(b)Departamento de Física, Universidad Técnica Federico Santa María, Valparaíso, Chile
- 145 Department of Physics, University of Washington, Seattle, WA, USA
- 146 Department of Physics and Astronomy, University of Sheffield, Sheffield, UK
- 147 Department of Physics, Shinshu University, Nagano, Japan
- 148 Department Physik, Universität Siegen, Siegen, Germany
- 149 Department of Physics, Simon Fraser University, Burnaby, BC, Canada
- 150 SLAC National Accelerator Laboratory, Stanford, CA, USA
- 151 Physics Department, Royal Institute of Technology, Stockholm, Sweden
- 152 Departments of Physics and Astronomy, Stony Brook University, Stony Brook, NY, USA
- 153 Department of Physics and Astronomy, University of Sussex, Brighton, UK
- 154 School of Physics, University of Sydney, Sydney, Australia
- 155 Institute of Physics, Academia Sinica, Taipei, Taiwan
- 156 ^(a)E. Andronikashvili Institute of Physics, Iv. Javakishvili Tbilisi State University, Tbilisi, Georgia; ^(b)High Energy Physics Institute, Tbilisi State University, Tbilisi, Georgia
- 157 Department of Physics, Technion, Israel Institute of Technology, Haifa, Israel
- 158 Raymond and Beverly Sackler School of Physics and Astronomy, Tel Aviv University, Tel Aviv, Israel
- 159 Department of Physics, Aristotle University of Thessaloniki, Thessaloniki, Greece
- 160 International Center for Elementary Particle Physics and Department of Physics, University of Tokyo, Tokyo, Japan
- 161 Graduate School of Science and Technology, Tokyo Metropolitan University, Tokyo, Japan
- 162 Department of Physics, Tokyo Institute of Technology, Tokyo, Japan
- 163 Tomsk State University, Tomsk, Russia
- 164 Department of Physics, University of Toronto, Toronto, ON, Canada
- 165 ^(a)TRIUMF, Vancouver, BC, Canada; ^(b)Department of Physics and Astronomy, York University, Toronto, ON, Canada
- 166 Division of Physics and Tomonaga Center for the History of the Universe, Faculty of Pure and Applied Sciences, University of Tsukuba, Tsukuba, Japan
- 167 Department of Physics and Astronomy, Tufts University, Medford, MA, USA
- 168 Department of Physics and Astronomy, University of California Irvine, Irvine, CA, USA
- 169 Department of Physics and Astronomy, University of Uppsala, Uppsala, Sweden
- 170 Department of Physics, University of Illinois, Urbana, IL, USA
- 171 Instituto de Física Corpuscular (IFIC), Centro Mixto Universidad de Valencia, CSIC, Valencia, Spain
- 172 Department of Physics, University of British Columbia, Vancouver, BC, Canada

- 173 Department of Physics and Astronomy, University of Victoria, Victoria, BC, Canada
- 174 Fakultät für Physik und Astronomie, Julius-Maximilians-Universität Würzburg, Würzburg, Germany
- 175 Department of Physics, University of Warwick, Coventry, UK
- 176 Waseda University, Tokyo, Japan
- 177 Department of Particle Physics, Weizmann Institute of Science, Rehovot, Israel
- 178 Department of Physics, University of Wisconsin, Madison, WI, USA
- 179 Fakultät für Mathematik und Naturwissenschaften, Fachgruppe Physik, Bergische Universität Wuppertal, Wuppertal, Germany
- 180 Department of Physics, Yale University, New Haven, CT, USA
- 181 Yerevan Physics Institute, Yerevan, Armenia
- ^a Also at Department of Physics, University of Malaya, Kuala Lumpur, Malaysia
- ^b Also at Borough of Manhattan Community College, City University of New York, NY, USA
- ^c Also at California State University, East Bay, USA
- ^d Also at Centre for High Performance Computing, CSIR Campus, Rosebank, Cape Town, South Africa
- ^e Also at CERN, Geneva, Switzerland
- ^f Also at CPPM, Aix-Marseille Université, CNRS/IN2P3, Marseille, France
- ^g Also at Département de Physique Nucléaire et Corpusculaire, Université de Genève, Genève, Switzerland
- ^h Also at Departament de Física de la Universitat Autònoma de Barcelona, Barcelona, Spain
- ⁱ Also at Departamento de Física Teórica y del Cosmos, Universidad de Granada, Granada (Spain), Spain
- ^j Also at Department of Applied Physics and Astronomy, University of Sharjah, Sharjah, United Arab Emirates
- ^k Also at Department of Financial and Management Engineering, University of the Aegean, Chios, Greece
- ^l Also at Department of Physics and Astronomy, University of Louisville, Louisville, KY, USA
- ^m Also at Department of Physics and Astronomy, University of Sheffield, Sheffield, UK
- ⁿ Also at Department of Physics, California State University, Fresno CA, USA
- ^o Also at Department of Physics, California State University, Sacramento CA, USA
- ^p Also at Department of Physics, King's College London, London, UK
- ^q Also at Department of Physics, Nanjing University, Nanjing, China
- ^r Also at Department of Physics, St. Petersburg State Polytechnical University, St. Petersburg, Russia
- ^s Also at Department of Physics, Stanford University, USA
- ^t Also at Department of Physics, University of Fribourg, Fribourg, Switzerland
- ^u Also at Department of Physics, University of Michigan, Ann Arbor MI, USA
- ^v Also at Dipartimento di Fisica E. Fermi, Università di Pisa, Pisa, Italy
- ^w Also at Giresun University, Faculty of Engineering, Giresun, Turkey
- ^x Also at Graduate School of Science, Osaka University, Osaka, Japan
- ^y Also at Hellenic Open University, Patras, Greece
- ^z Also at Horia Hulubei National Institute of Physics and Nuclear Engineering, Bucharest, Romania
- ^{aa} Also at II Physikalisches Institut, Georg-August-Universität Göttingen, Göttingen, Germany
- ^{ab} Also at Institutio Catalana de Recerca i Estudis Avancats, ICREA, Barcelona, Spain
- ^{ac} Also at Institut für Experimentalphysik, Universität Hamburg, Hamburg, Germany
- ^{ad} Also at Institute for Mathematics, Astrophysics and Particle Physics, Radboud University Nijmegen/Nikhef, Nijmegen, Netherlands
- ^{ae} Also at Institute for Particle and Nuclear Physics, Wigner Research Centre for Physics, Budapest, Hungary
- ^{af} Also at Institute of Particle Physics (IPP), Canada
- ^{ag} Also at Institute of Physics, Academia Sinica, Taipei, Taiwan
- ^{ah} Also at Institute of Physics, Azerbaijan Academy of Sciences, Baku, Azerbaijan
- ^{ai} Also at Institute of Theoretical Physics, Ilia State University, Tbilisi, Georgia
- ^{aj} Also at Istanbul University, Dept. of Physics, Istanbul, Turkey
- ^{ak} Also at LAL, Université Paris-Sud, CNRS/IN2P3, Université Paris-Saclay, Orsay, France
- ^{al} Also at Louisiana Tech University, Ruston LA, United States of America
- ^{am} Also at LPNHE, Sorbonne Université, Paris Diderot Sorbonne Paris Cité, CNRS/IN2P3, Paris, France
- ^{an} Also at Manhattan College, New York NY, USA
- ^{ao} Also at Moscow Institute of Physics and Technology State University, Dolgoprudny, Russia

^{ap} Also at National Research Nuclear University MEPhI, Moscow, Russia

^{aq} Also at Near East University, Nicosia, North Cyprus, Mersin, Turkey

^{ar} Also at Physikalisches Institut, Albert-Ludwigs-Universität Freiburg, Freiburg, Germany

^{as} Also at School of Physics, Sun Yat-sen University, Guangzhou, China

^{at} Also at The City College of New York, New York NY, United States of America

^{au} Also at The Collaborative Innovation Center of Quantum Matter (CICQM), Beijing, China

^{av} Also at Tomsk State University, Tomsk, and Moscow Institute of Physics and Technology State University, Dolgoprudny, Russia.

^{aw} Also at TRIUMF, Vancouver BC, Canada

^{ax} Also at Università di Napoli Parthenope, Napoli, Italy

*Deceased